NASA/TM–2013-218039

Entropy Stable Spectral Collocation Schemes for the Navier-Stokes Equations: Discontinuous Interfaces

Mark H. Carpenter
Langley Research Center, Hampton, Virginia

Travis C. Fisher
Sandia National Laboratories, Albuquerque, New Mexico

Eric J. Nielsen
Langley Research Center, Hampton, Virginia

Steven H. Frankel
Purdue University, West Lafayette, Indiana

September 2013

NASA STI Program . . . in Profile

Since its founding, NASA has been dedicated to the advancement of aeronautics and space science. The NASA scientific and technical information (STI) program plays a key part in helping NASA maintain this important role.

The NASA STI program operates under the auspices of the Agency Chief Information Officer. It collects, organizes, provides for archiving, and disseminates NASA's STI. The NASA STI program provides access to the NASA Aeronautics and Space Database and its public interface, the NASA Technical Report Server, thus providing one of the largest collections of aeronautical and space science STI in the world. Results are published in both non-NASA channels and by NASA in the NASA STI Report Series, which includes the following report types:

- TECHNICAL PUBLICATION. Reports of completed research or a major significant phase of research that present the results of NASA Programs and include extensive data or theoretical analysis. Includes compilations of significant scientific and technical data and information deemed to be of continuing reference value. NASA counterpart of peer-reviewed formal professional papers, but having less stringent limitations on manuscript length and extent of graphic presentations.

- TECHNICAL MEMORANDUM. Scientific and technical findings that are preliminary or of specialized interest, e.g., quick release reports, working papers, and bibliographies that contain minimal annotation. Does not contain extensive analysis.

- CONTRACTOR REPORT. Scientific and technical findings by NASA-sponsored contractors and grantees.

- CONFERENCE PUBLICATION. Collected papers from scientific and technical conferences, symposia, seminars, or other meetings sponsored or co-sponsored by NASA.

- SPECIAL PUBLICATION. Scientific, technical, or historical information from NASA programs, projects, and missions, often concerned with subjects having substantial public interest.

- TECHNICAL TRANSLATION. English-language translations of foreign scientific and technical material pertinent to NASA's mission.

Specialized services also include organizing and publishing research results, distributing specialized research announcements and feeds, providing information desk and personal search support, and enabling data exchange services.

For more information about the NASA STI program, see the following:

- Access the NASA STI program home page at *http://www.sti.nasa.gov*

- E-mail your question to help@sti.nasa.gov

- Fax your question to the NASA STI Information Desk at 443-757-5803

- Phone the NASA STI Information Desk at 443-757-5802

- Write to:
  STI Information Desk
  NASA Center for AeroSpace Information
  7115 Standard Drive
  Hanover, MD 21076-1320

NASA/TM–2013-218039

Entrophy Stable Spectral Collocation Schemes for Navier-Stokes Equations: Discontinuous Interfaces

Mark H. Carpenter
Langley Research Center, Hampton, Virginia

Travis C. Fisher
Sandia National Laboratories, Albuquerque, New Mexico

Eric J. Nielsen
Langley Research Center, Hampton, Virginia

Steven H. Frankel
Purdue University, West Lafayette, Indiana

National Aeronautics and
Space Administration

Langley Research Center
Hampton, Virginia 23681-2199

September 2013

Acknowledgments

Special thanks are extended to Dr. Mujeeb Malik for funding this work as part of the "Revolutionary Computational Aerosciences" project.

Available from:

NASA Center for AeroSpace Information
7115 Standard Drive
Hanover, MD 21076-1320
443-757-5802

Abstract

Nonlinear entropy stability and a summation-by-parts framework are used to derive provably stable, polynomial-based spectral collocation methods of arbitrary order. The new methods are closely related to discontinuous Galerkin spectral collocation methods commonly known as DGFEM, but exhibit a more general entropy stability property. Although the new schemes are applicable to a broad class of linear and nonlinear conservation laws, emphasis herein is placed on the entropy stability of the compressible Navier-Stokes equations.

Contents

1 Introduction

A current organizational research goal of NASA's *Revolutionary Computational AeroSciences* subproject of the Aeronautical Sciences Project is to develop next generation high-order numerical algorithms for use in large eddy simulations (LES) and hybrid Reynolds-averaged Navier-Stokes (RANS)-LES simulations of complex separated flow. These algorithms must be suitable for simulations of highly nonlinear next generation turbulence models across the subsonic, transonic and supersonic speed regimes.

Although high-order techniques are well suited for LES, most lack robustness when the solution contains discontinuities or even under-resolved physical features. Although a variety of mathematically rigorous stabilization techniques have been developed for second-order methods (e.g., total variation diminishing (TVD) limiters [1], and entropy stability [2]), extending these techniques to high-order formulations has been problematic. A typical consequence is loss of design order accuracy at local extrema or insufficient stabilization. It is possible by using essentially nonoscillatory (ENO) [3, 4] and weighted ENO (WENO) [5, 6] schemes, to achieve high-order design accuracy away from captured discontinuities, and maintain sharp "nearly monotone" captured shocks. Unfortunately, nonoscillatory schemes experience instabilities in less than ideal circumstances (i.e., curvilinear mapped grids or expansion of flows into vacuum). Because these schemes are largely based on stencil biasing heuristics rather than mathematical stability proofs and the theory that does exist is not sharp [7,8], there is little to guide further development efforts focused on alleviating the instabilities; that is, until recently.

Fisher and Carpenter [9,10] provide a general procedure for developing entropy conservative and entropy stable schemes of any order, for broad classes of spatial operators. The work generalizes entropy stability results appearing in the literature by several authors over the past two decades. A brief overview of the evolutionary developments of entropy stability is now presented. Nearly three decades ago, entropy conservative schemes that discretely satisfy an entropy conservation property

are constructed by Tadmor for second-order finite volume methods [2, 11]. These schemes were extended to high-order periodic domains by LeFloch and Rhode [12]. Finding a computationally friendly discrete entropy flux was a major obstacle that was alleviated recently for the Navier-Stokes equations through the work of Ismail and Roe [13]. A methodology for constructing entropy stable schemes satisfying a cell entropy inequality and capable of simulating flows with shocks in periodic domains was developed by Fjordholm et al. [14]. Recently, Fisher and Carpenter [9, 10] present multi-domain proofs of entropy conservation and stability based on diagonal norm summation-by-parts (SBP) operators, that yield entropy stable methods on finite domains. Generalization to arbitrary Cartesian domains follows immediately using simultaneous-approximation-term (SAT) penalty type interface conditions [15] between adjoining domains.

Although the primary focus of references [9,10] is entropy stable WENO finite-difference schemes, all proofs immediately generalize to a broad class of summation-by-parts (SBP-SAT) operators. Indeed, any spatial discretization that may be expressed as a non-dissipative, diagonal norm, SBP-SAT operator can be implemented in an entropy conservative and stable fashion. Thus, it is now possible to construct entropy conservative and stable formulations of arbitrary order for many popular discrete operators.

Spectral collocation operators are readily expressed in SBP-SAT form [16–19], although not all may be expressed as diagonal norm SBP operators; e.g., the mass matrix of a Chebyshev operator is full. Legendre collocation schemes, however, may be expressed as diagonal norm SBP operators, and therefore satisfy the sufficient conditions for an entropy stable implementation. Thus the focus herein is developing conservation form, entropy conservative, Legendre spectral collocation schemes for the Navier-Stokes equations.[1]

To place this work into the appropriate context, note that the SBP-SAT entropy stability proofs developed herein (and references [9, 10]), are not the first appearing in the high-order literature, although they do have some unique properties. Nonlinear analysis for the Navier-Stokes equations appears in the work of Hughes et al. [20] in the context of Galerkin and Petrov-Galerkin finite-element methods (FEM). Entropy stability of the FEM follows immediately by rotating the conservative equations into symmetric form followed by a conventional FEM implementation. Symmetrizing the equations, however, raises the question of whether the method is consistent with the Lax-Wendroff theorem. The SBP-SAT stability proofs are implemented in conservation form and do not have this ambiguity.

Likewise, entropy stability proofs for alternative nonlinear equations appear in many finite-element texts, e.g., see Hesthaven and Warburten [21] for a discussion of Burgers' equation. Extension to the compressible Navier-Stokes equations in conservation form, has not been forthcoming to our knowledge. Indeed, a fundamental obstacle in FEM proofs is the requirement for exact integration formulae, a feat that is all but impossible for the compressible Navier-Stokes equations. (Recasting the equations in entropy variables is not an option because of inconsistency with the Lax-Wendroff theorem.) Again, the SBP-SAT entropy stability proofs do not suffer these limitations.

The entropy stable discrete operators developed herein are an important step towards a provably stable simulation methodology of arbitrary order for complex geometries. All proofs generalized immediately to 3D via tensor product arithmetic. The extension of the entropy stable methods

[1] An entropy stable correction for these Legendre spectral collocation scheme follows immediately from the results in [9,10] (e.g., a dissipative shock capturing numerical method such as WENO), but this development effort is deferred to a later paper.

to generalized (3D) curvilinear coordinates and multi-domain configurations is included in a companion paper. Two major hurdles remain on the path towards L_2 stability of the compressible Navier-Stokes equations. First, well-posed physical boundary conditions are needed that preserve the entropy stability property of the interior operator. Second, a fully discrete operator is needed that preserves the semi-discrete entropy stability properties (e.g., the trapezoidal rule) [11], and maintains positivity of the density and temperature.

The organization of this paper is as follows. The theory of SBP-SAT operators and their relationship to polynomial spectral collocation formulations, is presented in Section 2. This discussion is tutorial in extent, and may be skipped by readers familiar with SBP-SAT nomenclature and operators. Section 3 presents an introduction to continuous entropy analysis followed by semi-discrete analysis that demonstrates the entropy-mimetic properties of diagonal norm SBP operators. The analysis is valid for arbitrarily high-order accurate Legendre spectral collocation operators. Section 4 presents inviscid and viscous coupling conditions used to connect adjoining elements. Details of the implementation of entropy conservative operators in the context of the compressible Euler and Navier-Stokes equations are provided in Section 5. Finally, the accuracy of the resulting high-order schemes are demonstrated in Section 6, and conclusions are discussed in Section 7.

2 Methodology

Consider the calorically perfect Navier-Stokes equations, which may be expressed in the form

$$\begin{aligned} q_t + (f^i)_{x_i} = (f^{(v)i})_{x_i}, \quad x \in \Omega, \quad t \in [0, \infty), \\ Bq = g_b, \quad x \in \partial\Omega, \quad t \in [0, \infty), \\ q(x, 0) = g_0(x), \quad x \in \Omega, \end{aligned} \tag{2.1}$$

where the Cartesian coordinates, $x = (x_1, x_2, x_3)^T$, and time, t, are independent variables, and index sums are implied. The vectors q, f^i, and $f^{(v)i}$ are the conserved variables, the conserved inviscid fluxes and viscous fluxes, respectively. Without loss of generality, a three dimensional box

$$\Omega = [x_1^L, x_1^H] \times [x_2^L, x_2^H] \times [x_3^L, x_3^H]$$

is chosen as our computational domain with $\partial\Omega$ representing the boundary of the domain. The boundary vector, g_b, is assumed to contain well-posed Dirichlet/Neumann data. We have omitted a detailed description of the three-dimensional Navier-Stokes equations, which may be found elsewhere [22].

2.1 Summation-by-parts Operators

2.1.1 First Derivative

First derivative operators that satisfy the summation-by-parts (SBP) convention, discretely mimic the integration-by-parts condition

$$\int_{x_L}^{x_R} \phi q_x \, \mathrm{d}x = \phi q|_{x_L}^{x_R} - \int_{x_L}^{x_R} \phi_x q \, \mathrm{d}x. \tag{2.2}$$

This mimetic property is achieved by constructing the first derivative approximation, $\mathcal{D}\boldsymbol{\phi}$, with an operator in the form

$$\begin{gathered}\mathcal{D}=\mathcal{P}^{-1}\,\mathcal{Q},\quad \mathcal{P}=\mathcal{P}^{T},\quad \boldsymbol{\zeta}^{T}\mathcal{P}\boldsymbol{\zeta}>0,\quad \boldsymbol{\zeta}\neq\mathbf{0},\\ \mathcal{Q}^{T}=\mathcal{B}-\mathcal{Q},\quad \mathcal{B}=\operatorname{diag}\left(-1,0,\ldots,0,1\right).\end{gathered}\tag{2.3}$$

While it is not true in general that $\mathcal{P}$ is diagonal, herein the focus is exclusively on diagonal norm SBP operators, based on fixed element-based polynomials. The matrix $\mathcal{P}$ may be thought of as a mass matrix in the context of Galerkin finite-elements (FEM), incorporates the local grid spacing into the derivative definition. The nearly skew-symmetric matrix, $\mathcal{Q}$, is an undivided differencing operator where all rows sum to zero and the first and last column sum to -1 and 1, respectively. The accuracy of the first derivative operator, $\mathcal{D}$, may be expressed as

$$\phi_x(\mathbf{x})=\mathcal{D}\phi+\mathcal{T}_{(p+1)},\tag{2.4}$$

where $\mathcal{T}_{(p+1)}$ is the truncation error of the approximation, and p is the order of the polynomial. Integration in the approximation space is conducted using an inner product with the appropriate integration weights contained in the norm $\mathcal{P}$,

$$\int_{x_L}^{x_R}\phi q_x\,\mathrm{d}x\approx\boldsymbol{\phi}^{T}\mathcal{P}\mathcal{D}\mathbf{q},\quad \boldsymbol{\phi}=\left(\phi(x_1),\phi(x_2),\ldots,\phi(x_N)\right)^{T}.\tag{2.5}$$

Using the definition in 2.3, the SBP property is demonstrated,

$$\boldsymbol{\phi}^{T}\mathcal{P}\mathcal{P}^{-1}\mathcal{Q}\mathbf{q}=\boldsymbol{\phi}^{T}\left(\mathcal{B}-\mathcal{Q}^{T}\right)\mathbf{q}=\phi_N q_N-\phi_1 q_1-\boldsymbol{\phi}^{\boldsymbol{T}}\mathcal{D}^{T}\mathcal{P}\mathbf{q}.\tag{2.6}$$

The specific operators used in this work is shown in Appendix A.

2.1.2 The Second Derivative

The viscous approximations are written in general as

$$\left(\vartheta(x)q_x(\mathbf{x})\right)_x=\mathcal{D}_2(\vartheta)\mathbf{q}+\mathcal{T}_p^{(v)},\tag{2.7}$$

also satisfy the SBP condition. Integration by parts yields

$$\int_{x_L}^{x_R}\phi\left(\vartheta q_x\right)_x\,\mathrm{d}x=\phi\vartheta q_x|_{x_L}^{x_R}-\int_{x_L}^{x_R}\phi_x\vartheta q_x\,\mathrm{d}x.\tag{2.8}$$

The second derivative variable coefficient operator resulting from two applications of the first derivative may be manipulated for diagonal norm, $\mathcal{P}$, into the expression

$$\begin{gathered}\mathcal{D}_2(\vartheta)=\mathcal{P}^{-1}\left(-\mathcal{D}^{T}\mathcal{P}[\vartheta]\mathcal{D}+\mathcal{B}[\vartheta]\mathcal{D}\right),\quad \mathcal{D}^{T}\mathcal{P}[\vartheta]\mathcal{D}=\left(\mathcal{D}^{T}\mathcal{P}[\vartheta]\mathcal{D}\right)^{T},\quad [\vartheta]=\operatorname{diag}\left(\vartheta(\mathbf{x})\right),\\ \boldsymbol{\zeta}^{T}\left(\mathcal{D}^{T}\mathcal{P}[\vartheta]\mathcal{D}\right)\boldsymbol{\zeta}\geq 0,\quad \boldsymbol{\zeta}^{T}[\vartheta]\boldsymbol{\zeta}\geq 0,\quad \forall\boldsymbol{\zeta}.\end{gathered}\tag{2.9}$$

The $\mathcal{P}$-norm inner product yields the expression

$$\boldsymbol{\phi}^{T}\mathcal{P}\mathcal{P}^{-1}\left(-\mathcal{D}^{T}\mathcal{P}[\vartheta]\mathcal{D}+\mathcal{B}[\vartheta]\mathcal{D}\right)\mathbf{q}=\boldsymbol{\phi}^{T}\mathcal{B}[\vartheta]\mathcal{D}\mathbf{q}-\boldsymbol{\phi}^{T}\left(\mathcal{D}^{T}\mathcal{P}[\vartheta]\mathcal{D}\right)\mathbf{q}\tag{2.10}$$

which is the form used to show stability of the viscous terms. It is clear that the continuous interface terms are mimicked. Likewise, based on the definition 2.9 the expression,

$$\int_{x_L}^{x_R} \phi_x \vartheta q_x \, \mathrm{d}x \approx \boldsymbol{\phi}^T \left(\mathcal{D}^T \mathcal{P}[\vartheta] \mathcal{D} \right) \mathbf{q}$$

follows immediately.

2.1.3 Complementary Grids

Most existing entropy analysis is performed in indicial notation on a staggered set of solution and flux points. For example, Tadmor's telescoping entropy flux relation (fully defined in section 3.2.2) is written as

$$(w_{i+1} - w_i)^T \bar{f}_i = \tilde{\psi}_{i+1} - \tilde{\psi}_i,$$

and relates solution point data $w_i, w_{i+1}, \tilde{\psi}_i, \tilde{\psi}_{i+1}$ with a flux $\bar{f}_i$ located between the grid points. Conventional SBP operators are not directly applicable to this form of analysis; generalized operators suitable for a staggered grid implementation are now developed. The new operators satisfy a generalized summation-by-parts property.

Define on the interval $-1 \leq x \leq 1$, the vectors of discrete solution points

$$\mathbf{x} = [x_1, x_1, \cdots, x_{N-1}, x_N]^T \quad ; \quad -1 \leq x_1, x_2, \cdots, x_{N-1}, x_N \leq 1 \,. \tag{2.11}$$

Since the approximate solution is constructed at these points, they are denoted the *solution points*. It is useful to define a set of intermediate points prescribing bounding control volumes about each solution point. These $(N+1)$ points are denoted *flux points* as they are similar in nature to the control volume edges employed in the finite volume method. The distribution of the flux points depends on the discretization operator. The spacing between the flux points is implicitly contained in the norm $\mathcal{P}$; the diagonal elements of $\mathcal{P}$ are equal to the spacing between flux points,

$$\begin{gathered} \bar{\mathbf{x}} = (\bar{x}_0, \bar{x}_1, \ldots \bar{x}_N)^T, \quad \bar{x}_0 = x_1, \quad \bar{x}_N = x_N, \\ \bar{x}_i - \bar{x}_{i-1} = \mathcal{P}_{(i)(i)}, \quad i = 1, 2, \ldots, N. \end{gathered} \tag{2.12}$$

In operator notation, this is equivalent to

$$\Delta \bar{\mathbf{x}} = \mathcal{P}\mathbf{1} \quad ; \quad \mathbf{1} = (1, 1, \ldots, 1)^T \tag{2.13}$$

where Δ is as defined in equation 2.16. Note that in 2.12, the first and last flux points are coincident with the first and last solution points, which enables the endpoint fluxes to be consistent,

$$\bar{f}_0 = f(q_1), \quad \bar{f}_N = f(q_N). \tag{2.14}$$

This duality is needed to define unique operators and is important in proving entropy stability.

2.1.4 Telescopic Flux Form

All SBP derivative operators, $\mathcal{D}$, can be manipulated into the telescopic flux form,

$$f_x(\mathbf{q}) = \mathcal{P}^{-1}\mathcal{Q}\mathbf{f} + \mathcal{T}_{(p+1)} \;=\; \mathcal{P}^{-1}\Delta\overline{\mathbf{f}} + \mathcal{T}_{(p+1)}. \tag{2.15}$$

where the $N \times (N+1)$ matrix Δ is

$$\Delta = \begin{pmatrix} -1 & 1 & 0 & 0 & 0 & 0 \\ 0 & -1 & 1 & 0 & 0 & 0 \\ 0 & 0 & \ddots & \ddots & 0 & 0 \\ 0 & 0 & 0 & -1 & 1 & 0 \\ 0 & 0 & 0 & 0 & -1 & 1 \end{pmatrix}, \tag{2.16}$$

that calculates the undivided difference of the two adjacent fluxes. All conservative and accurate flux gradients may be constructed in the form of 2.15 for all SBP operators, $\mathcal{Q}$, a fact that is reiterated in the following lemma presented without proof. (The original proof appears in reference [23]).

Lemma 2.1. *All differentiation matrices that satisfy the SBP convention given in eq. (2.3) are telescoping operators in the norm $\mathcal{P}$.*

This telescopic flux form admits a generalized SBP property. All SBP operators defined in equation 2.3 can be manipulated to transfer the action of the discrete derivative onto a test function with an equivalent order of approximation. The telescopic flux form defined in equation 2.15 combined with the flux consistency condition results in a more generalized relation,

$$\boldsymbol{\phi}^T\mathcal{P}\mathcal{P}^{-1}\Delta\overline{\mathbf{f}} = \boldsymbol{\phi}^T(\tilde{\mathcal{B}} - \tilde{\Delta})\overline{\mathbf{f}} = f(q_N)\phi_N - f(q_1)\phi_1 - \boldsymbol{\phi}\tilde{\Delta}\overline{\mathbf{f}}, \tag{2.17}$$

where

$$\tilde{\Delta} = \begin{pmatrix} 0 & -1 & 0 & 0 & 0 & 0 \\ 0 & 1 & -1 & 0 & 0 & 0 \\ 0 & 0 & \ddots & \ddots & 0 & 0 \\ 0 & 0 & 0 & 1 & -1 & 0 \\ 0 & 0 & 0 & 0 & 1 & 0 \end{pmatrix}, \quad \tilde{\mathcal{B}} = \begin{pmatrix} -1 & 0 & 0 & 0 & 0 & 0 \\ 0 & 0 & 0 & 0 & 0 & 0 \\ 0 & 0 & \ddots & \ddots & 0 & 0 \\ 0 & 0 & 0 & 0 & 0 & 0 \\ 0 & 0 & 0 & 0 & 0 & 1 \end{pmatrix},$$

and

$$\frac{1}{\delta x}\boldsymbol{\phi}^T\tilde{\Delta} = \boldsymbol{\phi}_x^T + \mathcal{O}(N^{-1}).$$

This is equivalent to the commonly used explanation of summation-by-parts in indicial form,

$$\sum_{i=1}^{N}\phi_i\left(\bar{f}_i - \bar{f}_{i-1}\right) = f(q_N)\phi_N - f(q_1)\phi_1 - \sum_{i=1}^{N-1}\bar{f}_i\left(\phi_{i+1} - \phi_i\right). \tag{2.18}$$

The action of the derivative is still moved onto the test function but at first order accuracy. Note that although this generalized property is used herein to construct entropy conservative fluxes, it is also instrumental for satisfying the Lax-Wendroff theorem [24] in weak form.

Likewise, the variable coefficient viscous operators presented in Section 2.1.2 may be expressed in the form

$$(\vartheta q_x(\mathbf{x}))_x \approx \mathcal{P}^{-1}\left(-\mathcal{D}^T\mathcal{P}[\vartheta]\mathcal{D} + \mathcal{B}[\vartheta]\mathcal{D}\right)\mathbf{q} = \mathcal{P}^{-1}\Delta\overline{\mathbf{f}}^{(v)}, \tag{2.19}$$

and satisfy a telescoping conservation property which is identical to that of the inviscid terms.

2.1.5 The Semi-Discrete Operator

Based on the previous discussion of SBP operators and their equivalent telescoping form, the semi-discrete form of equation 2.1 becomes

$$\begin{gathered}\mathbf{q}_t \;=\; -\mathcal{D}_i[\mathbf{f}^i(v)] + \mathcal{D}_i[c]_{ij}\mathcal{D}_j\mathbf{q}) + \mathcal{P}^{-1}\mathbf{g}_b, \;=\; \mathcal{P}^{-1}\Delta_i\left(-\overline{\mathbf{f}}^i + \overline{\mathbf{f}}^{(v)i}\right) + \mathcal{P}^{-1}\mathbf{g}_b, \\ \mathbf{q}(x,0) = g_0(x), \quad x \in \Omega,\end{gathered} \tag{2.20}$$

with $\mathbf{g}_b$ containing the enforcement of boundary conditions. Full implementation details, including the viscous Jacobian $[c]_{ij}$ tensors are included in previous works [23, 25] and elsewhere [26–30].

Remark. It is not necessary to implement an SBP scheme in flux form, but is the natural form to add dissipation while retaining consistency with the Lax Wendroff theorem [23]. Furthermore, the semi-discrete entropy analysis presented in Section 5.1.3 relies on the existence of the flux form.

2.2 Spectral Discretization Operators

Spectral collocation methods are commonly implemented on computational grids based on the nodes of Gauss-quadrature formulas (i.e., Gauss, Gauss Radau, or Gauss Lobatto (GL)). These smooth but nonuniform grids are highly clustered at the boundaries of the domain, in stark contrast to the uniform grids used in conventional finite difference methods.

The numerical methods developed herein are all collocated at the Legendre Gauss-Labotto Legendre (LGL) points, and include both end points of the interval. This distribution that includes the end points, allows the operators to be written in terms of flux differences, analogous to a finite volume method and consistent with equations 2.17 and 2.19. The complete discretization operator for the $p = 4$ element is illustrated in Figure 1.

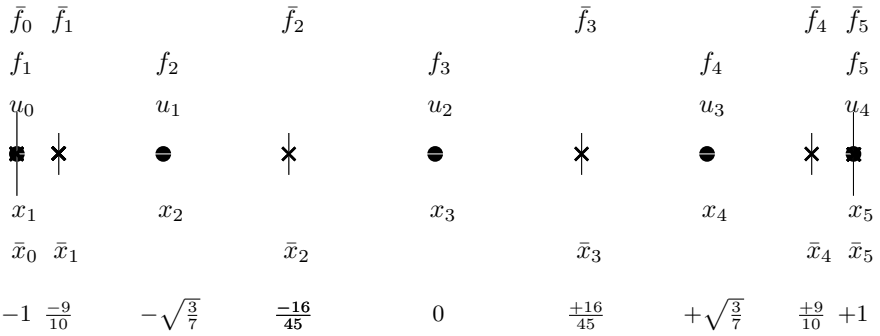

Figure 1. The one-dimensional discretization for $p = 4$ Legendre collocation is illustrated. Solution points are denoted by $\bullet$ and flux points are denoted by $\times$.

2.2.1 Lagrange Polynomials

Define the Lagrange polynomials on the discrete points $\mathbf{x}$ as

$$\begin{gathered}\hat{L}(x) = (x - x_2)(x - x_3)...(x - x_{n-2})(x - x_{N-1}) \\ L_1(x) = \tfrac{(1-x)\hat{L}(x)}{2\hat{L}(-1)} \quad ; \quad L_n(x) = \tfrac{(1+x)\hat{L}(x)}{2\hat{L}(+1)} \quad ; \quad L_j(x) = \tfrac{(1-x^2)\hat{L}(x)}{(x-x_j)\hat{L}'(x_j)} \qquad 2 \le j \le N-1\end{gathered} \tag{2.21}$$

With a slight abuse of notation, define the *vector* of Lagrange polynomials as

$$\mathbf{L}(x) \quad = \quad [L_1(x), L_2(x), \cdots, L_{N-1}(x), L_N(x)]^T \tag{2.22}$$

2.3 Differentiation

Assume that a smooth and (infinitely) differentiable function, $f(x)$, is defined on the interval $-1 \leq x \leq 1$. Reading the function f and derivative f' at the discrete points, $\mathbf{x}$, yields the vectors

$$\begin{array}{rcl} \mathbf{f}(\mathbf{x}) & = & [f(x_1), f(x_2), \cdots, f(x_{N-1}), f(x_N)]^T \, ; \\ \mathbf{f}'(\mathbf{x}) & = & [f'(x_1), f'(x_2), \cdots, f'(x_{N-1}), f'(x_N)]^T \, . \end{array} \tag{2.23}$$

The interpolation polynomial, $f_N(x)$, that collocates $f(x)$ at the points $\mathbf{x}$ is given by the contraction

$$f(x) \; \approx \; f_{(N-1)}(x) \; = \; [\mathbf{L}(x)]^T \mathbf{f}(\mathbf{x}) \, . \tag{2.24}$$

Derivative operators expressed in terms of the Lagrange polynomials on the interval are derived in the following theorem, presented without proof. (The proof appears in many texts, e.g., reference [31].)

Theorem 2.2. *The derivative operator that exactly differentiates an arbitrary n^{th} order polynomial at the collocation points, $\mathbf{x}$, is*

$$\mathcal{D} \; = \; [L_j^{'}(x_i)] \, . \tag{2.25}$$

The elements of $\mathcal{D}$ are $d_{i,j}$ for $\quad 1 \leq i, j \leq n \; .$

An equivalent representation of the differentiation operator may also be used, that satisfies all the requirements for being an SBP operator (but in general will not be a diagonal norm SBP operator).

Theorem 2.3. *The derivative operator that exactly differentiates an arbitrary p^{th} order polynomial ($p = N - 1$) at the collocation points, $\mathbf{x}$, may be expressed as*

$$\mathcal{D} \; = \; \mathcal{P}^{-1} \, \mathcal{Q} \, . \tag{2.26}$$

Proof. First note that in addition to expression (2.33), the exact derivative $\frac{df(x)}{dx}$ of the function $f(x)$ may be approximated by

$$f'(x) \; \approx \; \frac{df_n(x)}{dx} \; = \; [\mathbf{L}(x)]^T \mathbf{f}'(\mathbf{x}) \, . \tag{2.27}$$

The Galerkin statement demands that the integral error between the two expressions be orthogonal to the basis set which in this case are the Lagrange polynomials $\mathbf{L}(x)$. This statement may be expressed as

$$\int_{-1}^{1} \mathbf{L}(x) \left([\mathbf{L}(x)]^T \mathbf{f}'(\mathbf{x}) \; - \; [\mathbf{L}^{'}(x)]^T \mathbf{f}(\mathbf{x}) \right) \, dx \; = \; 0 \, , \tag{2.28}$$

or in the equivalent form

$$\hat{\mathcal{P}} \, \mathbf{f}'(\mathbf{x}) \; = \; \mathcal{Q} \, \mathbf{f}(\mathbf{x}) \, , \tag{2.29}$$

with

$$\hat{\mathcal{P}} \;=\; \int_{-1}^{1} \mathbf{L}(x)[\mathbf{L}(x)]^T\, dx \qquad ; \qquad \mathcal{Q} \;=\; \int_{-1}^{1} \mathbf{L}(x)[\mathbf{L}^{'}(x)]^T\, dx\,. \tag{2.30}$$

Equation (2.26) follows immediately when $\hat{\mathcal{P}}$ is symmetric positive definite (SPD), and therefore invertible.

The symmetry of $\hat{\mathcal{P}}$ follows immediately from definition (2.30). Positive definiteness of $\hat{\mathcal{P}}$ is established by pre- and post-multiply $\hat{\mathcal{P}}$ by an arbitrary nonzero discrete vector, ψ, which yields the expression

$$\psi^T\hat{\mathcal{P}}\psi \;=\; \int_{-1}^{1} \psi^T\mathbf{L}(x)[\mathbf{L}(x)]^T\psi\, dx \;=\; \int_{-1}^{1} \psi(x)^2\, dx \tag{2.31}$$

that is strictly greater than zero, unless ψ is the null vector. Thus, the matrix $\hat{\mathcal{P}}$ is SPD, therefore invertible, and (2.26) follows immediately. □

Remark Once the invertibility of $\hat{\mathcal{P}}$ established, equation (2.26) may be proven directly by showing that $\hat{\mathcal{P}}\,\mathcal{D} \;=\; \mathcal{Q}$.

A proof that $\mathcal{Q}$ is nearly skew-symmetric is as follows.

Theorem 2.4. *The matrix* $\mathcal{Q} \;=\; \int_{-1}^{1} \mathbf{L}(x)[\mathbf{L}^{'}(x)]^T\, dx$ *is structurally of the form*

$$\mathcal{Q} + \mathcal{Q}^T = \mathcal{B}\,. \tag{2.32}$$

Thus, by virtue of the structure of $\hat{\mathcal{P}}$ and $\mathcal{Q}$, the differentiation operator, $\mathcal{D}$, is indeed an SBP operator defined by 2.3.

Proof. Integrating by parts the definition of $\mathcal{Q}$ yields the expression

$$\mathcal{Q} \;=\; \int_{-1}^{1} \mathbf{L}(x)[\mathbf{L}^{'}(x)]^T\, dx \;=\; \mathbf{L}(x)(+1)[\mathbf{L}(x)(+1)]^T - \mathbf{L}(x)(-1)[\mathbf{L}(x)(-1)]^T - \int_{-1}^{1} \mathbf{L}^{'}(x)[\mathbf{L}(x)]^T\, dx. \tag{2.33}$$

All Lagrange polynomials based on the Gauss-Labotto collocation points vanish on the boundaries for $1 < i, j < N$. Thus, the boundary matrices reduce to the form

$$\mathbf{L}(x)(+1)[\mathbf{L}(x)(+1)]^T - \mathbf{L}(x)(-1)[\mathbf{L}(x)(-1)]^T \;=\; \delta_{i,N}\delta_{j,N} - \delta_{i,1}\delta_{j,1}.$$

Writing equation 2.33 in indicial nomenclature leads to $q_{i,j} + q_{j,i} = \delta_{i,N}\delta_{j,N} - \delta_{i,1}\delta_{j,1}$ which is the desired result. □

2.3.1 Collocation

A Legendre collocation operator may be constructed by approximating the integrals in equations 2.30, 2.31 and 2.4 by the LGL quadrature formula. Let $\eta \;=\; (\eta_1, \eta_2, \cdots \eta_{N-1}, \eta_N)$ be the nodes of the LGL quadrature formula (i.e., the zeroes of the polynomial $P_{n-1}^{'}(x)(1-x^2)$ [31]), and let ω_l, $1 \le l \le N$ be the quadrature weights.

Next, define new mass and stiffness matrices $\mathcal{P}$ and $\mathcal{Q}_c$ by the expressions

$$\mathcal{P} \;=\; \textstyle\sum_l \mathbf{L}(\eta_l;\mathbf{x})[\mathbf{L}(\eta_l;\mathbf{x})]^T\eta_l\, dx \qquad ; \qquad \mathcal{Q}_c \;=\; \textstyle\sum_l \mathbf{L}(\eta_l;\mathbf{x})[\mathbf{L}^{'}(\eta_l;\mathbf{x})]^T\eta_l\, dx\,. \tag{2.34}$$

The matrix $\mathcal{P}$ is SPD for any $\mathbf{x}$. The proof is structurally equivalent to the Galerkin proof given in equation 2.31 and is omitted.

Note that in general, $\hat{\mathcal{P}} \neq \mathcal{P}$. The LGL formula is exact for polynomials of degree $2p-1$ but $\int_{-1}^{1} \mathbf{L}(x)[\mathbf{L}(x)]^T \, dx$ is of degree $2p$. Thus, the integration differs for the highest order term (i.e., $2p^{th}$). Indeed, the two matrix norms differ by a rank one perturbation, i.e $\hat{\mathcal{P}} = \mathcal{P} + \gamma_p \mathcal{D}^p \mathbf{e_0} [\mathcal{D}^p \mathbf{e_0}]^T$ where $\mathbf{e_0} = [1, 0, \cdots, 0]^T$, $\mathcal{D}^p$ is the highest derivative supported by the polynomial, and γ_p depends on polynomial order.

The matrices $\mathcal{Q}$ and $\mathcal{Q}_c$ are equivalent. This follows from the fact of the two matrices are defined by the polynomials $\int_{-1}^{1} \mathbf{L}(x)[\mathbf{L}'(x)]^T \, dx$ that have a combined rank of $2p-1$. Therefore, integration is exact when using the LGL integration formula.

The uniqueness of the differentiation matrix $\mathcal{D}$ yields the expression

$$\mathcal{D} = \hat{\mathcal{P}}^{-1} \mathcal{Q} = \mathcal{P}^{-1} \mathcal{Q} \, .$$

This statement does not contradict the fact that $\hat{\mathcal{P}} \neq \mathcal{P}$. Indeed, expanding the $\hat{\mathcal{P}}^{-1}$ using the Sherman-Morrison formula demonstrates that the difference in the inverses lies in the null space of the singular $\mathcal{D}$ matrix.

2.3.2 Diagonal Norm SBP Operators

Theorem 2.5. *The matrix $\mathcal{P}$ is diagonal for collocations points located at the LGL quadrature points, i.e., $\mathbf{x} = \eta$. Furthermore the diagonal coefficients of $\mathcal{P}$ are the integration weights ω_l, $1 \leq l \leq N$ used in the quadrature.*

Proof. Recall that the Lagrange polynomials evaluated at the knot points satisfy the property $L_i(x_j) = \delta_{i,j}$. Thus, the result follows immediately from the definition of the norm $\mathcal{P} = \sum_l \mathbf{L}(\eta_l; \mathbf{x})[\mathbf{L}(\eta_l; \mathbf{x})]^T \eta_l$. □

2.4 SAT Penalty Boundary and Interface Conditions

The imposition of boundary and interface conditions is of critical importance in all numerical methods for partial differential equations on finite domains. The manner in which these conditions are imposed greatly affects the stability and accuracy of solutions. Accurate, stable, and conservative interface coupling techniques are essential in multi-domain settings and become critical as the domains (i.e., elements) are refined in size.[2]

A straightforward method that permits formal analysis and maintains design-order accuracy is the SAT penalty method [26–30]. The approximate spatial integration of the semi-discretization in 2.20,

$$\frac{d}{dt} \mathbf{1}^T \mathcal{P} \mathbf{q} = \bar{f}_0 - \bar{f}_N + \bar{f}_N^{(v)} - \bar{f}_0^{(v)} + \mathbf{1}^T \left(\mathbf{g}_b + \mathbf{g}_I \right), \tag{2.35}$$

illustrates the purpose of the penalty, that may be thought of as replacing some of the computed data in the approximation with known data from the boundary condition to specify a mathematically well-posed problem.

[2]Indeed, the ratio of interior to interface terms remains constant independent of resolution in spectral element discretizations; the ratio goes to zero in a multi-block finite-difference discretization.

3 Entropy Stable Spectral Collocation: Single Domain

3.1 Continuous Analysis

3.1.1 Smooth Solutions

Consider a nonlinear system of equations (e.g., the Navier-Stokes equations given in 2.1) and assume that the solution is smooth for all time. The objective is to bound the solution as sharply as possible. A quadratic or otherwise convex extension of the original equations is sought (the existence is in general not guaranteed), that when integrated over the domain depends only on boundary data and dissipative terms. Fortunately, the Navier-Stokes equations have a convex extension, referred to as the entropy function that provides a mechanism for proving stability of the nonlinear system.

Definition 3.1. *A scalar function $S = S(q)$ is an entropy function of equation 2.1 if it satisfies the following conditions:*

- *The function $S(q)$ is convex and when differentiated, simultaneously contracts all spatial fluxes as follows*
$$S_q f^i_{x_i} \;=\; S_q f^i_q q_{x_i} \;=\; F^i_q q_{x_i} \;=\; F^i_{x_i} \quad ; \quad i = 1, \cdots, d \tag{3.1}$$
for each spatial coordinate, d. The components of the contracting vector, S_q, are the entropy variables denoted as $w^T = S_q$. $F^i(q)$ are the entropy fluxes in the i-direction.

- *The entropy variables, w, symmetrize equation 2.1 if w assumes the role of a new dependent variable (i.e., $q = q(w)$). Expressing equation 2.1 in terms of w is*
$$q_t + (f^i)_{x_i} - (f^{(v)i})_{x_i} \;=\; q_w w_t + (f^i_w) w_{x_i} - (\hat{c}_{ij} w_{x_j})_{x_i} = 0 \quad ; \quad i = 1, \cdots, d \tag{3.2}$$
with the symmetry conditions: $q_w = [q_w]^T$, $f^i_w = {f^i_w}^T$, $\hat{c}_{ij} = \hat{c}^T_{ji}$.

Because the entropy is convex, the Hessian $S_{qq} = w_q$ is symmetric positive definite,

$$\zeta^T S_{qq} \zeta > 0, \quad \forall \zeta \neq 0, \tag{3.3}$$

and yields a one-to-one mapping from conservation variables, q, to entropy variables, $w^T = S_q$. Likewise, w_q is SPD because $q_w = {w_q}^{-1}$ and SPD matrices are invertible. The entropy and corresponding entropy flux are often denoted an entropy–entropy flux pair, (S, F). Likewise, the potential and the corresponding potential flux (defined next) are denoted a potential–potential flux pair, (φ, ψ) [11].

The symmetry of the matrices q_w and f^i_w, indicates that the conservation variables, q, and fluxes, f^i, are Jacobians of scalar functions with respect to the entropy variables,

$$q^T = \varphi_w, \quad [f^i]^T = \psi^i_w, \tag{3.4}$$

where the nonlinear function, φ, is called the potential and ψ^i are called the potential fluxes [11]. Just as the entropy function is convex with respect to the conservative variables (S_{qq} is positive definite), the potential function is convex with respect to the entropy variables.

The two elements of Definition 3.1 are closely related, as is shown by Godunov [32] and Mock [33]. Godunov proves that:

Theorem 3.1. *If equation 2.1 can be symmetrized by introducing new variables w, and q is a convex function of φ, then an entropy function $S(q)$ is given by*

$$\varphi = w^T q - S, \tag{3.5}$$

and the entropy fluxes $F^i(q)$ satisfy

$$\psi^i = w^T f^i - F^i. \tag{3.6}$$

Mock proves the converse to be true:

Theorem 3.2. *If $S(q)$ is an entropy function of equation 2.1; then $w^T = S_q$ symmetrizes the equation.*

See reference [34] for a detailed summary of both proofs.

Entropy analysis is now applied to the Navier-Stokes equations to determine the limits of non-linear stability.

Contracting equation 2.1 with the entropy variables results in the differential form of the entropy equation,

$$S_q q_t + S_q f(q)_{x_i} = S_t + F_{x_i} = S_q f^{(v)}_{x_i} = \left(w^T f^{(v)}\right)_{x_i} - w^T_{x_i} f^{(v)i} = \left(w^T f^{(v)}\right)_{x_i} - w^T_{x_i} \hat{c}_{ij} w_{x_i} \tag{3.7}$$

Integrating equation 3.7 over the domain yields a global conservation statement for the entropy in the domain

$$\frac{d}{dt} \int_\Omega S \, \mathrm{d}x_i = \left[w^T f^{(v)} - F\right]_{\partial\Omega} - \int_\Omega w^T_{x_j} \hat{c}_{ij} w_{x_i} \, \mathrm{d}x_i. \tag{3.8}$$

It is shown elsewhere [9,10] that $\hat{c}_{ij}$ in the last term in the integral are positive semi-definite. Note that the entropy can only increase in the domain based on data that convects and diffuses through the boundaries. The sign of the entropy change from viscous dissipation is always negative.

Thus, the entropy equation derived in 3.8 is the convex extension of the original Navier-Stokes equations, and the entropy function serves as an estimator of stability of the system.

3.1.2 Discontinuous Solutions

The Euler terms in equation 2.1 (the convective terms to the left of the equal sign) admit discontinuous solutions in finite time even for smooth initial and boundary data. Thus, weak solutions to the integral form of equation 2.1 are appropriate for these situations. Although equation 3.8 is an integral statement of entropy conservation, it is not strictly valid in the presence of discontinuities, because it does not accurately account for the dissipation of entropy at the discontinuity (i.e., shocks).[3] Although the precise amount of entropy dissipated at a shock is not known apriori, what is known is the sign of the jump in entropy. Thus, a general (yet somewhat ambiguous) statement of the conservation of entropy in the domain is

$$\frac{d}{dt} \int_\Omega S \, \mathrm{d}x_i \leq \left[w^T f^{(v)} - F\right]_{\partial\Omega} - \int_\Omega w^T_{x_j} \hat{c}_{ij} w_{x_i} \, \mathrm{d}x_i. \tag{3.9}$$

[3]Note that the mathematical entropy has the opposite sign from thermodynamic entropy in gas dynamics.

Weak solutions in general may not be unique [24,35]. In these cases, Equation 3.9 is used to identify spurious solutions that violate the entropy condition from those that are physically admissible. Entropy analysis is valid for nonlinear equations and even those that admit discontinuous solutions; it is more generally applicable than linear energy analysis and gives a stronger stability estimate.

3.2 Semi-Discrete Entropy Analysis

The semi-discrete entropy estimate is achieved by mimicking term by term the continuous estimate given in equation 3.8. The nonlinear analysis begins by contracting the entropy variables, $\mathbf{w}^T$, with the semi-discrete equation 2.20. (For clarity of presentation, but without loss of generality, the derivation is simplified to one spatial dimension. Tensor product algebra allows the results to extended directly to three-dimensions.) The resulting global equation that governs the semi-discrete decay of entropy is given by

$$\mathbf{w}^T \mathcal{P} \mathbf{q}_t + \mathbf{w}^T \Delta \overline{\mathbf{f}} = \mathbf{w}^T \Delta \overline{\mathbf{f}}^{(v)} + \mathbf{w}^T \mathbf{g}_b, \tag{3.10}$$

where

$$\mathbf{w} = \left(w(q_1)^T, w(q_2)^T, \ldots, w(q_N)^T \right)^T,$$

the vector of entropy variables. Each semi-discrete term is now analyzed to demonstrate that it mimics the corresponding term in continuous entropy estimate, provided that a diagonal norm SBP operator is used. The form of the penalty terms is presented in a later section 4.

3.2.1 Time Derivative

The time derivative is by definition in mimetic form for diagonal norm SBP operators. Arbitrary diagonal matrices commute, so the pointwise definition of entropy

$$w_i^T (q_i)_t \;=\; (S_i)_t, \quad \forall i.$$

yields the expression

$$\mathbf{w}^T \mathcal{P} \mathbf{q}_t \;=\; \mathbf{1}^T \mathcal{P} \mathbf{w}^T \mathbf{q}_t \;=\; \mathbf{1}^T \mathcal{P} S_u \mathbf{q}_t \;=\; \mathbf{1}^T \mathcal{P} \mathbf{S}_t.$$

3.2.2 Inviscid Flux Conditions

The inviscid portion of equation 3.10 is entropy conservative if it satisfies

$$\mathbf{w}^T \Delta \overline{\mathbf{f}} = F(q_N) - F(q_1) = \mathbf{1}^T \Delta \overline{\mathbf{F}}. \tag{3.11}$$

Recall that $\mathbf{w}$ and $\overline{\mathbf{f}}, \overline{\mathbf{F}}$ are defined at the solution points and flux points, respectively. One plausible solution to equation 3.11 is a pointwise relation between solution and flux-point data, which telescopes across the domain and produces the entropy fluxes at the boundaries. Tadmor [11] developed such a solution based on second-order centered operators. Herein, this solution is generalized for Legendre spectral collocation operators of any order.

Theorem 3.3. *The local conditions*

$$(w_{i+1} - w_i)^T \, \bar{f}_i = \tilde{\psi}_{i+1} - \tilde{\psi}_i, \quad i = 1, 2, \ldots, N-1 \quad ; \quad \tilde{\psi}_1 = \psi_1, \quad \tilde{\psi}_N = \psi_N \tag{3.12}$$

when summed, telescope across the domain and satisfy the entropy conservative condition given in equation 3.11. The potentials $\tilde{\psi}_{i+1}$ and $\tilde{\psi}_i$ need not be the pointwise ψ_{i+1} and ψ_i, respectively. A flux that satisfies this condition given in equation 3.12 is denoted $\overline{\mathbf{f}}^{(S)}$.

Proof. Substituting the definition for generalized summation-by-parts in Section 2.1.4, $\Delta = \tilde{\mathcal{B}} - \tilde{\Delta}$, into the global entropy conservation condition in equation 3.11 yields

$$\mathbf{w}^T \tilde{\mathcal{B}} \overline{\mathbf{f}} - \mathbf{w}^T \tilde{\Delta} \overline{\mathbf{f}} - \mathbf{1}^T \tilde{\mathcal{B}} \overline{\mathbf{F}} + \mathbf{1}^T \tilde{\Delta} \overline{\mathbf{F}} = \mathbf{w}^T \tilde{\mathcal{B}} \overline{\mathbf{f}} - \mathbf{1}^T \tilde{\mathcal{B}} \overline{\mathbf{F}} - \mathbf{w}^T \tilde{\Delta} \overline{\mathbf{f}} = 0. \tag{3.13}$$

The boundary terms in 3.13 may be reorganized as

$$\mathbf{w}^T \tilde{\mathcal{B}} \overline{\mathbf{f}} - \mathbf{1}^T \tilde{\mathcal{B}} \overline{\mathbf{F}} = (w_N^T f_N - F_N) - (w_1^T f_1 - F_1) = \psi_N - \psi_1 = \tilde{\boldsymbol{\psi}}^T \tilde{\mathcal{B}} \bar{\mathbf{1}}, \tag{3.14}$$

where ψ_1 and ψ_N represent the potential flux defined in equation 3.6. Defining $[\overline{\mathbf{f}}]$ as a diagonal $(N+1) \times (N+1)$ matrix containing the elements of $\overline{\mathbf{f}}$, and substituting equations 3.13 and 3.14 into 3.11 yields

$$\left(\tilde{\boldsymbol{\psi}}^T \tilde{\mathcal{B}} - \mathbf{w}^T \tilde{\Delta} [\overline{\mathbf{f}}] \right) \bar{\mathbf{1}} = 0.$$

Substituting the equality $\tilde{\boldsymbol{\psi}}^T \tilde{\mathcal{B}} \bar{\mathbf{1}} = \tilde{\boldsymbol{\psi}}^T \tilde{\Delta} \bar{\mathbf{1}}$ into the left hand side of the equation yields

$$\left(\tilde{\boldsymbol{\psi}}^T \tilde{\Delta} - \mathbf{w}^T \tilde{\Delta} [\overline{\mathbf{f}}] \right) \bar{\mathbf{1}} = 0. \tag{3.15}$$

This is satisfied by the vector sufficient condition,

$$\tilde{\boldsymbol{\psi}}^T \tilde{\Delta} = \mathbf{w}^T \tilde{\Delta} [\overline{\mathbf{f}}], \quad \tilde{\psi}_1 = \psi_1, \quad \tilde{\psi}_N = \psi_N. \tag{3.16}$$

A pointwise examination of the vector condition yields the desired result. □

Note that Tadmor arrives at the condition $\tilde{\boldsymbol{\psi}} = \boldsymbol{\psi}$ because of an assumption on the form of $\overline{\mathbf{F}}$ [11]. In the generalized condition derived in equation 3.16 it is unnecessary to define $\tilde{\psi}$ in the domain interior. This generality is important because the entropy conservative fluxes needed for high-order methods do not satisfy Tadmor's original two point form [12].

The local conditions defined in equation 3.12 are sufficient for three-point, second-order centered discretizations. The entropy conservative flux is constructed at each flux point, $\bar{f}_i$, from solution point data obtained from the two adjacent solution points, i and $i+1$. The resulting operator telescopes across the domain when contracted with the entropy variables.

Likewise, equation 3.12 is generalizable to coarser grids using the notion of Richardson extrapolation; e.g., two point, second order, skew-symmetric operators spanning $5pt$, $7pt$, $9pt$, $\cdots$. Thus, if a high-order derivative operator may be constructed from linear combinations of these elemental second-order operators, then high-order accuracy is achieved that ensures entropy consistency. (Schemes of this class are devised for periodic domains by LeFloch and Rhode [12], and extended to high-order periodic domains by LeFloch and Rhode [12].)

The matrix footprint of any spectral collocation operator is dense and involves $(p+1)^2$ individual terms. Neither of the two previous approaches extend in general to these dense operators. A different strategy for constructing high-order entropy conservative fluxes is presented in reference [9, 10], and utilizes linear combinations of two-point entropy conservative fluxes, combined

using the coefficients in the SBP matrix $\mathcal{Q}$. This new approach follows immediately from the generalized telescoping structural properties of diagonal norm SBP operators given in section 2.1.4. Because is requires only the existence of a two-point entropy conservative flux formula and the coefficients of the $\mathcal{Q}$, it is valid for any SBP operator which satisfies the constraints given in equation 2.3. Thus, it is valid for Legendre spectral collocation operators.

The proofs of this alternative approach for building entropy conservative operators of any order are quite involved. For brevity only two of the theorems are included herein. Interested readers should consult references [9, 10] for details.

The first theorem establishes the accuracy of the new fluxes: that a high-order flux constructed from a linear combination of two-point entropy conservative fluxes retains the design order of the original discrete operator for any diagonal norm SBP matrix $\mathcal{Q}$.

Theorem 3.4. *A two-point entropy conservative flux can be extended to high order with formal boundary closures by using the form*

$$\bar{f}_i^{(S)} = \sum_{k=i+1}^{N} \sum_{\ell=1}^{i} 2q_{(\ell,k)} \bar{f}_S \left(q_\ell, q_k\right), \quad 1 \leq i \leq N-1, \tag{3.17}$$

when the two-point non-dissipative function from Tadmor [11] is used

$$\bar{f}_S \left(q_k, q_\ell\right) = \int_0^1 g\left(w(q_k) + \xi \left(w(q_\ell) - w(q_k)\right)\right) \mathrm{d}\xi, \quad g(w(u)) = f(u). \tag{3.18}$$

The coefficient, $q_{(k,\ell)}$, corresponds to the (k, ℓ) row and column in $\mathcal{Q}$, respectively.

Proof. To show the accuracy of approximation, the flux difference is expressed as

$$\bar{f}_i^{(S)} - \bar{f}_{i-1}^{(S)} = \sum_{k=i+1}^{N} \sum_{\ell=1}^{i} 2q_{(\ell,k)} \bar{f}_S \left(u_\ell, u_k\right) - \sum_{k=i}^{N} \sum_{\ell=1}^{i-1} 2q_{(\ell,k)} \bar{f}_S \left(u_\ell, u_k\right), \quad 2 \leq i \leq N-1.$$

that may be manipulated into the form (see references [9, 10])

$$\bar{f}_i^{(S)} - \bar{f}_{i-1}^{(S)} = \sum_{j=1}^{N} 2q_{(i,j)} \bar{f}_S(u_i, u_j), \quad 1 \leq i \leq N. \tag{3.19}$$

This form facilitates an analysis by Taylor series at every solution point by using the expression for the two-point fluxes given in equation 3.18. The remainder of the proof is presented elsewhere [9, 10]. □

The second theorem establishes that the linear combination does indeed preserve the property of entropy stability for any arbitrary diagonal norm SBP matrix $\mathcal{Q}$.

Theorem 3.5. *A two-point high-order entropy conservative flux satisfying equation 3.12 with formal boundary closures can be constructed using equation 3.17,*

$$\bar{f}_i^{(S)} = \sum_{k=i+1}^{N} \sum_{\ell=1}^{i} 2q_{(\ell,k)} \bar{f}_S \left(q_\ell, q_k\right), \quad 1 \leq i \leq N-1,$$

where $f_S(q_\ell, q_k)$ is any two-point non-dissipative function that satisfies the entropy conservation condition

$$(w_\ell - w_k)^T \bar{f}_S(q_\ell, q_k) = \psi_\ell - \psi_k. \tag{3.20}$$

The high-order entropy conservative flux satisfies an additional local entropy conservation property,

$$\mathbf{w}^T \mathcal{P}^{-1} \Delta \bar{\mathbf{f}}^{(S)} = \mathcal{P}^{-1} \Delta \overline{\mathbf{F}} = F_x(\mathbf{q}) + \mathcal{T}_d, \tag{3.21}$$

or equivalently,

$$w_i^T \left(\bar{f}_i^{(S)} - \bar{f}_{i-1}^{(S)} \right) = \left(\bar{F}_i - \bar{F}_{i-1} \right), \quad 1 \le i \le N, \tag{3.22}$$

where

$$\bar{F}_i = \sum_{k=i+1}^{N} \sum_{\ell=1}^{i} q_{(\ell,k)} \left[(w_\ell + w_k)^T \bar{f}_S(q_\ell, q_k) - (\psi_\ell + \psi_k) \right], \quad 1 \le i \le N-1. \tag{3.23}$$

Proof. For brevity, the proof is not included herein, but is reported elsewhere [9, 10]. □

*R*emark. The existence of a local second-order entropy flux satisfying the two point shuffle relation given in equation 3.20 is a very strong constraint, and has until recently been a computation bottleneck [13].

Remark. The entropy consistency proof is satisfied for all two-point fluxes that satisfy 3.20. The accuracy proof is proven only for fluxes in the integral form 3.18. Currently, the proof does not extend to any flux satisfying 3.20, so such fluxes should be validated for accuracy independent of Theorem 3.4.

In summary, Theorems 3.4 and 3.5, guarantee that the extension of the two-point flux given in equation 3.17, is a high-order accurate entropy conservative discretization of the conservation law.

3.3 Entropy Stability of the Euler Equations

Tadmor [11] identifies three "tools of the trade" in the analysis of entropy stability: *comparison arguments*, a homotropy approach, and kinetic formulations. In a comparison approach, the entropy dissipation generated by the primary scheme is compared with the baseline entropy of a scheme known to be at least entropy conservative. If the dissipation is less than the entropy conservative datum, then more dissipation is necessary. Conditions that guarantee entropy stability are developed in references [9, 10], and extend directly to this work. Stabilization of the inviscid terms is the topic of ongoing work.

3.4 Entropy Stable Viscous Terms

Using the formalism introduced in Section 2.1.2, viscous terms are derived that discretely mimics the continuous entropy properties. As with the continuous estimate, the proof requires the viscous fluxes to be written as functions of the discrete gradients of the entropy variables,

$$\begin{aligned} (\hat{c}_{ii} w_x)_x = \mathcal{P}^{-1} \Delta \bar{\mathbf{f}}^{(v)} = \mathcal{D}_2(\hat{c}_{ii}) \mathbf{w} + \mathcal{T}_p, \\ \mathcal{D}_2(\hat{c}_{ii}) \mathbf{w} = \mathcal{P}^{-1} \left(-\mathcal{D}^T \mathcal{P}[\hat{c}_{ii}] \mathcal{D} + \mathcal{B}[\hat{c}_{ii}] \mathcal{D} \right) \mathbf{w}. \end{aligned} \tag{3.24}$$

The accuracy requirements are automatically satisfied. The coefficient matrix $[\hat{c}_{ii}]$ is positive semi-definite because it is constructed from block-diagonal combinations of positive semi-definite matrices.

The contribution of the viscous terms to the semi-discrete entropy decay rate is

$$\mathbf{w}^T \Delta\overline{\mathbf{f}}^{(v)} = \mathbf{w}\mathcal{B}[\hat{c}_{ii}]\mathcal{D}\mathbf{w} - (\mathcal{D}\mathbf{w})^T\mathcal{P}[\hat{c}_{ii}](\mathcal{D}\mathbf{w}). \tag{3.25}$$

The last term is negative semi-definite. As with the continuous estimate given in 3.8, only the boundary term can produce a growth of the entropy, and thus the approximation of the viscous terms is entropy stable. (Wellposed boundary conditions bound these terms.)

The high-order entropy stable viscous terms described in equations 3.24 and 3.25 first appear in a companion work [9,10], that focuses primarily on the entropy stability of WENO finite-difference operators. Unlike multi-domain finite-difference formulations, spectral element operators have the potential to superconverging from p to $p+1$, with the appropriate choice of viscous interface coupling terms. Thus, a slightly modified discretization of the viscous terms is adopted herein.

4 Entropy Stable Spectral Collocation: Multi-Domains and Discontinuous Interfaces

Design order consistent, conservative interface treatments that are provably entropy stable are developed next. Two popular techniques for coupling interfaces are the discontinuous and continuous approaches. The focus herein is on the discontinuous approach.

Numerous discontinuous coupling approaches exist for spectral element operators. See reference [36] for a review of the (weak form) finite element literature or [18] for a general treatment of strong form collocation approaches. The advantage of discontinuous approaches is that each domain may be treated individually. The inviscid terms are typically coupled across the interface through a Riemann solver, a technique that ensures conservation and which provides a necessary mechanism for dissipating unresolved modes in the simulation. Likewise, numerous approaches exist for coupling the viscous terms across interfaces, but two of the more popular are the Local Discontinuous Galerkin (LDG) FEM approach proposed by Cockburn and Shu [37], and the second technique proposed by Bassi and Rebay [38]. The present work develops a new entropy stable LDG approach based on the strong (differential) form of the governing equations.

4.1 Navier-Stokes in One Spatial Dimension

For clarity of presentation we analyze the one-dimensional case. Extension to three spatial dimensions is straightforward although algebraically involved. The inviscid and viscous penalties are developed separately to guarantee an entropy stable inviscid penalty in the limit of vanishing viscosity.

A spectral collocation approximation for the Navier-Stokes equations, including interface coupling terms, motivated by the LDG FEM approach is

$$
\begin{array}{rll}
\mathcal{P}_l[\frac{\partial q_l}{\partial t} + \Delta\overline{\mathbf{f}}_l - \mathcal{D}_l\hat{c}_{ii}\boldsymbol{\Xi}_l] = & [+\overline{\mathbf{f}}_i^{(-)} - \mathbf{f}^{ssr}(q^{(-)},q^{(+)}) + L_{00}(w_i^{(-)} - w_i^{(+)}) + L_{01}(\Xi_i^{(-)} - \Xi_i^{(+)})] & \mathbf{e_i^{(-)}} \\
\mathcal{P}_l(\boldsymbol{\Xi}_l - \mathcal{D}_l w) = & +L_{10}(w_i^{(-)} - w_i^{(+)}) & \mathbf{e_i^{(-)}} \\
\mathcal{P}_r[\frac{\partial q_r}{\partial t} + \Delta\overline{\mathbf{f}}_r - \mathcal{D}_r\hat{c}_{ii}\boldsymbol{\Xi}_r] = & [-\overline{\mathbf{f}}_i^{(+)} + \mathbf{f}^{ssr}(q^{(-)},q^{(+)}) + R_{00}(w_i^{(+)} - w_i^{(-)}) + R_{01}(\Xi_i^{(+)} - \Xi_i^{(-)})] & \mathbf{e_i^{(+)}} \\
\mathcal{P}_r(\boldsymbol{\Xi}_r - \mathcal{D}_r w) = & +R_{10}(w_i^{(+)} - w_i^{(-)}) & \mathbf{e_i^{(+)}}
\end{array}
\tag{4.1}
$$

with the subscripts l, r denoting the "left,right" elements (subdomains). The subscript i denotes an interface quantity with the superscripts "(-),(+)" denoting the collocated values on the left and right side of the interface, respectively. The flux $\mathbf{f}^{ssr}(q^{(-)},q^{(+)})$ is an entropy stable reconstructed flux.

Theorem 4.1. *The approximation (4.1) of the one-dimensional Navier-Stokes equations is entropy stable if the reconstructed flux $\mathbf{f}^{ssr}(q^{(-)},q^{(+)})$ and the viscous matrix parameters L_{00},L_{01},L_{10}, R_{00},R_{01},R_{10} satisfy the following conditions. The entropy stable reconstruction $\mathbf{f}^{ssr}(q^{(-)},q^{(+)})$ must be more dissipative than the entropy conservative reconstruction. A sufficient condition is the use of dissipation of the form*

$$
\left(w^{(+)} - w^{(-)}\right)^T \mathbf{f}^{ssr}(q^{(-)},q^{(+)}) \;=\; \psi^{(+)} - \psi^{(-)} \quad - \Gamma_{diss}. \tag{4.2}
$$

where Γ_{diss} is an interface term which is uniformly dissipative (e.g., Lax-Friedrichs dissipation), or zero.

The viscous parameters must satisfy the conditions.

$$
L_{00} \;=\; R_{00} \;\leq\; 0 \quad ; \quad R_{01} \;=\; +L_{01} \;+\; \bar{c}_{ii} \quad ; \quad R_{10} \;=\; L_{10} \;+\; \bar{c}_{ii} \quad ; \quad L_{10} \;=\; -L_{01} \;-\; \bar{c}_{ii} \quad ; \tag{4.3}
$$

where symmetric dissipation matrix $\bar{c}_{ii}$ is defined as

$$
\bar{c}_{ii} \;=\; \tfrac{1}{2}(\hat{c}_{ii}^{(-)} \;+\; \hat{c}_{ii}^{(+)}) \quad . \tag{4.4}
$$

Finally, suitable boundary conditions and initial data must be provided.

Proof. Entropy stability of (4.1) follows if the interface treatment at $x = x_i$ is more dissipative than the entropy conservative interface treatment. The farfield boundary penalties are assumed to be stable, allowing separate analysis of the interface terms.

The entropy method is used to prove the stability of equation (4.1). Multiplying the two discrete equations in the left subdomain by w_l^T and $(\hat{c}_{iil}\,\Xi_l)^T$, respectively, and the two discrete equations in the right subdomain by w_r^T and $(\hat{c}_{iir}\,\Xi_r)^T$, respectively, and then summing the four equations and collecting terms results in the expression

$$
\tfrac{d}{dt}[\|S_l\|^2_{\mathcal{P}_l} + \|S_r\|^2_{\mathcal{P}_r}] \;+\; 2[\,\|\sqrt{\hat{c}_{iil}}\,\Xi_l\|^2_{\mathcal{P}_l} + \|\sqrt{\hat{c}_{iir}}\,\Xi_r\|^2_{\mathcal{P}_r}] \;=\; \Upsilon_i \tag{4.5}
$$

where

$$
\begin{array}{rcl}
\Upsilon_i & = & [2w_l\hat{c}_{iil}\,\Xi_l \;-\; F(q)]_{-1}^{i_-} \;+\; [2w_r\hat{c}_{iir}\,\Xi_r \;-\; F(q)]_{i_+}^{1} \\
& + & w_i^{(-)}(f(q_i^{(-)}) - \mathbf{f}^{ssr}(q^{(-)},q^{(+)})) - w_i^{(+)}(F(q_i^{(+)}) - \mathbf{f}^{ssr}(q^{(-)},q^{(+)})) \\
& + & 2L_{00}\;w_i^{(-)}\,[w_i^{(-)} - w_i^{(+)}] \;+\; 2L_{01}\;w_i^{(-)}\,[\Xi_i^{(-)} - \Xi_i^{(+)}] \;+\; 2L_{10}\;\Xi_i^{(-)}\,[w_i^{(-)} - w_i^{(+)}] \\
& + & 2R_{00}\;w_i^{(+)}\,[w_i^{(+)} - w_i^{(-)}] \;+\; 2R_{01}\;w_i^{(+)}\,[\Xi_i^{(+)} - \Xi_i^{(-)}] \;+\; 2R_{10}\;\Xi_i^{(+)}\,[w_i^{(+)} - w_i^{(-)}]
\end{array}
\tag{4.6}
$$

The viscous dissipation terms $\|\sqrt{\hat{c}_{iil}}\,\Xi_l\|^2_{\mathcal{P}_l}$ and $\|\sqrt{\hat{c}_{iir}}\,\Xi_r\|^2_{\mathcal{P}_r}$ are uniformly dissipative. Thus, entropy stability of equation (4.5) follows immediately if the term Υ_i is dissipative. Note that Υ_i is composed of both inviscid and viscous terms; i.e., $\Upsilon_i = \Upsilon_i^{Invisid} + \Upsilon_i^{Viscous}$. The inviscid and viscous terms are bounded individually to guarantee that the inviscid terms are stable in the limit of $Re \to \infty$.

Inviscid Stability

The inviscid interface terms in Υ_i are

$$\begin{aligned} \Upsilon_i^{Invisid} &= F(q_i^{(+)}) - F(q^{(-)}) \\ &+ w_i^{(-)}(f(q_i^{(-)}) - \mathbf{f}^{ssr}(q^{(-)}, q^{(+)})) - w_i^{(+)}(F(q_i^{(+)}) - \mathbf{f}^{ssr}(q^{(-)}, q^{(+)})) \end{aligned} \tag{4.7}$$

Substituting the definitions for the entropy fluxes

$$F(q_i^{(+)}) = w_i^{(+)} f(q_i^{(+)}) + \psi^{(+)} \quad ; \quad F(q_i^{(-)}) = w_i^{(-)} f(q_i^{(-)}) + \psi^{(-)} \,,$$

into equation 4.7 yields the equation

$$\Upsilon_i^{Invisid} = \left(w^{(+)} - w^{(-)}\right)^T \mathbf{f}^{ssr}(q^{(-)}, q^{(+)}) - (\psi^{(+)} - \psi^{(-)}) \tag{4.8}$$

that is a dissipative term provided that condition 4.2 is met.

Viscous Stability

Stability of the viscous interface terms is proven by collecting all remaining terms in 4.6 and expressing them as a matrix contraction $\Upsilon_i^{Viscous} = \mathcal{T}_i^T M_i \mathcal{T}_i$, where

$$\mathcal{T}_i = \left[w_i^{(-)} w_i^{(+)} \Xi^{(-)}{}_i \Xi^{(+)}{}_i\right]^T$$

and

$$M_i = \begin{bmatrix} (+2L_{00}) & -(L_{00}+R_{00}) & (c_{iil}+L_{01}+L_{10}) & -(L_{01}+R_{10}) \\ -(L_{00}+R_{00}) & (+2R_{00}) & -(R_{01}+L_{10}) & (-c_{iir}+R_{01}+R_{10}) \\ (c_{iil}+L_{01}+L_{10}) & -(R_{01}+L_{10}) & -(2\alpha_l c_{iil}) & 0 \\ -(L_{01}+R_{10}) & (-c_{iir}+R_{01}+R_{10}) & 0 & -(2\alpha_r c_{iir}) \end{bmatrix} . \tag{4.9}$$

Note that the matrix M_i is symmetric by construction. Stability of the interface follows immediately if M_i is negative semi-definite, a matrix property that is easily established by testing for the existence of a Cholesky factorization. The admissible values of the six viscous parameters $L_{00}--R_{10}$ are determined by requiring strictly negative diagonal pivots during the Cholesky factorization of M_i which yields the desired result. □

Conservation is a desirable property of any numerical method based on the strong form of the equations, and guarantees that convergent solutions satisfy the weak form of the governing equations away from discontinuities. The conservation property is established by multiplying equation 4.1 by an arbitrary smooth test function, and then transferring the action of the derivative operator (via matrix manipulations) over to the test function.

All inviscid terms at the interface vanish immediately by the specific choice of the penalty, provided that the test function is continuous across the interface. The viscous condition

$$L_{01} = R_{01} - \hat{c}_{ii}$$

is necessary for the approximation (4.1) to retain conservation (in the $\mathcal{P}$ norm) across the interface. Note that this condition is also identified as a necessary constraint during the Cholesky factorization of the matrix M_i.

4.1.1 Inviscid interface dissipation

The entropy stable flux $\mathbf{f}^{ssr}(q^{(-)}, q^{(+)})$ used in equation 3.12 is composed of the sum of an entropy conservative flux $\mathbf{f}^{sr}(q^{(-)}, q^{(+)})$ and a dissipation term Γ_{diss}. Lax-Friedrichs dissipation is perhaps the simplest means of stabilizing the interface. The resulting flux may be expressed as

$$\begin{aligned} \mathbf{f}^{ssr}(q^{(-)}, q^{(+)}) \;=\; \mathbf{f}^{sr}(q^{(-)}, q^{(+)}) \;+\; \tfrac{\lambda_{max}}{2}(w^{(-)} - w^{(+)})\,, \\ \lambda = [\tfrac{1}{2}((u^{(-)})^4 + (c^{(+)})^4 + (u^{(-)})^4 + (c^{(+)})^4)]^{\frac{1}{4}}\,. \end{aligned} \tag{4.10}$$

A flux that includes dissipation in this form is denoted an *entropy stable Lax-Friedrichs* flux. Note that this form differs from the conventional Lax-Friedrichs flux by replacing the linear average of the interface fluxes $\frac{1}{2}(f(q^{(-)}) + f(q^{(-)}))$, with the nonlinear average entropy conservative flux $\mathbf{f}^{sr}(q^{(-)}, q^{(+)})$. In practice, the dissipation term may be scaled by any positive number. The resulting term produces in the entropy estimate as the interface terms are contracted against the entropy variables is of the form

$$-\lambda(w^{(-)} - w^{(+)})^2 \tag{4.11}$$

Lax-Friedrichs dissipation overly damps the convective waves at the interface. A more refined approach to dissipate scales each characteristic component based on the magnitude of its eigenvalue. A flux that includes dissipation of this form is denoted an *entropy stable characteristic* flux, and is implemented as

$$\begin{aligned} \mathbf{f}^{ssr}(q^{(-)}, q^{(+)}) \;=\; \mathbf{f}^{sr}(q^{(-)}, q^{(+)}) \;+\; 1/2\mathcal{Y}|\lambda|\mathcal{Y}^T(w^{(-)} - w^{(+)})\,, \\ (\hat{f})_q \;=\; \mathcal{Y}\lambda\mathcal{Y}^T \quad ; \quad q_w \;=\; \mathcal{Y}\mathcal{Y}^T \end{aligned} \tag{4.12}$$

Note that the relation $q_w = \mathcal{Y}\mathcal{Y}^T$ is achieved by an appropriate scaling of the rotation eigenvectors. See the work of Merriam [39] for more details.

5 Entropy analysis for the Navier-Stokes equations

5.1 Euler and Navier-Stokes Equations

The end goal of this work is to simulate the Navier-Stokes equations in a stable and efficient manner. Toward this end, the application of entropy stable inviscid and viscous terms are detailed in this section. The conservative variables for the Navier-Stokes equations are

$$q = (\rho, \rho\upsilon_1, \rho\upsilon_2, \rho\upsilon_3, \rho E)^T\,, \tag{5.1}$$

where ρ denotes density, $\upsilon = (\upsilon_1, \upsilon_2, \upsilon_3)^T$ is the velocity vector, and E is the specific total energy. The convective fluxes are

$$f^i = (\rho\upsilon_i, \rho\upsilon_i\upsilon_1 + \delta_{i1}p, \rho\upsilon_i\upsilon_2 + \delta_{i2}p, \rho\upsilon_i\upsilon_3 + \delta_{i3}p, \rho\upsilon_i H)^T\,, \tag{5.2}$$

where p represents pressure, $H = E + p/\rho$ is the specific total enthalpy, and δ_{ij} is the Kronecker delta. The viscous flux terms are

$$f^{(v)i} = (0, \tau_{i1}, \tau_{i2}, \tau_{i3}, \tau_{ji}\upsilon_j - q_i)^T, \tag{5.3}$$

where the shear stress is

$$\tau_{ij} = \mu\left((\upsilon_i)_{x_j} + (\upsilon_j)_{x_i} - \delta_{ij}\frac{2}{3}(\upsilon_\ell)_{x_\ell}\right), \tag{5.4}$$

and the heat flux is

$$q_i = -\kappa T_{x_i}. \tag{5.5}$$

T denotes the static temperature, with $\mu = \mu(T)$ and $\kappa = \kappa(T)$ the dynamic viscosity and thermal conductivity, respectively.

The viscous terms may also be expressed as

$$f^{(v)i} = c_{ij}q_{x_j}, \tag{5.6}$$

which is a convenient form for entropy analysis. The constitutive relations for a perfect gas are

$$h = H - \frac{1}{2}\upsilon_j\upsilon_j = c_pT, \tag{5.7}$$

where c_p is the constant specific heat, and

$$p = \rho RT, \quad R = \frac{R_u}{MW}, \tag{5.8}$$

where R_u is the universal gas constant and MW is the molecular weight of the gas. The speed of sound for a perfect gas is

$$c = \sqrt{\gamma RT}, \quad \gamma = \frac{c_p}{c_p - R}. \tag{5.9}$$

In the entropy analysis that follows, the definition of the thermodynamic entropy is the explicit form,

$$s = \frac{R}{\gamma - 1}\log\left(\frac{T}{T_0}\right) - R\log\left(\frac{\rho}{\rho_0}\right). \tag{5.10}$$

where T_0 and ρ_0 are the reference temperature and density, respectively.

5.1.1 Entropy Analysis

In the Navier-Stokes equations, entropy stability is not the same as full non-linear stability. Nevertheless, entropy stability gives a stronger stability estimate than linear energy stability, and in many ways is easier to apply. In this section, the continuous entropy stability analysis is conducted first to illustrate the entropy characteristics of the governing equations. Discrete spatial operators are derived next, via semi-discrete entropy analysis, that mimic these continuous properties.

The entropy–entropy flux pair for the Navier-Stokes equations is

$$S = -\rho s, \quad F^i = -\rho\upsilon_i s, \tag{5.11}$$

and the potential–potential flux pair is

$$\varphi = \rho R, \quad \psi^i = \rho v_i R. \tag{5.12}$$

Note again that the mathematical entropy has the opposite sign of the thermodynamic entropy. To avoid confusion, herein entropy refers to the mathematical entropy unless otherwise noted. The entropy variables using the pair in 5.11 are

$$w = S_q^T = \left(\frac{h}{T} - s - \frac{v_j v_j}{2T}, \frac{v_1}{T}, \frac{v_2}{T}, \frac{v_3}{T}, -\frac{1}{T} \right)^T, \tag{5.13}$$

and may be shown to have a one-to-one mapping with the conservative variables provided $\rho, T > 0$. Expressly:

$$\zeta^T S_{qq} \zeta^T > 0, \quad \forall \zeta \neq 0, \quad \rho, T > 0.$$

This restriction is what makes the entropy proof fail to be a true measure of nonlinear stability. Another mechanism must be employed to bound ρ and T away from zero to guarantee stability.

The entropy equation is found by premultiplying the Navier-Stokes equations with the transpose of the entropy variables,

$$S_q q_t + S_q (f^i)_{x_i} = S_t + F^i_{x_i} = w^T \left(c_{ij} q_w w_{x_j} \right)_{x_i} = \left(w^T c_{ij} q_w w_{x_j} \right)_{x_i} - w^T_{x_i} c_{ij} q_w w_{x_j}, \tag{5.14}$$

where the viscous terms satisfy

$$c_{ij} q_w = \hat{c}_{ij} = \hat{c}^T_{ji}, \quad \zeta_{x_i} \hat{c}_{ij} \zeta_{x_j} \geq 0, \quad \forall \zeta, \tag{5.15}$$

provided

$$T > 0, \quad \mu(T) > 0, \quad \kappa(T) > 0.$$

The total entropy decay rate is found by integrating 5.14 over space,

$$\frac{d}{dt} \int_\Omega S \, \mathrm{d}V = \int_{\partial\Omega} \left(w^T \hat{c}_{ij} w_{x_j} - F^i \right) \partial S^i - \int_\Omega w^T_{x_i} \hat{c}_{ij} w_{x_j} \, \mathrm{d}V. \tag{5.16}$$

5.1.2 Discretization Notes

To facilitate the extension of the entropy stable methods to the three-dimensional equations, we define the three-dimensional nomenclature and examine the general form of the semi-discretization. The semi-discrete form of 2.1 is

$$\mathbf{q}_t + \sum_{i=1}^{3} \mathcal{P}^{-1}_{x_i} \Delta_{x_i} \left(\overline{\mathbf{f}}^i - \overline{\mathbf{f}}^{(v)i} \right) = \sum_{i=1}^{3} \mathcal{P}^{-1}_{x_i} \left(\mathbf{g}^i_b + \mathbf{g}^i_I \right). \tag{5.17}$$

The solution vector is ordered as

$$\mathbf{q} = \left(u(x_{(1)(1)(1)})^T, u(x_{(1)(1)(2)})^T, \ldots, u(x_{(N_1)(N_2)(N_3)})^T \right)^T.$$

The roman superscript indices on the flux in 5.17 indicate the direction of the flux, and parenthetic superscripts indicate the type of flux, i.e. V for viscous and S for entropy conservative.

5.1.3 Entropy Stable Spatial Discretization

The inviscid terms in the discretization of the Navier-Stokes equations are calculated according to equations 3.17 and 3.18, by using the two-point entropy conservative flux of Ismail and Roe [13],

$$\begin{aligned}
\bar{f}^j_S(q_i, q_{i+1}) &= \left(\hat{\rho}\hat{v}_j, \hat{\rho}\hat{v}_j\hat{v}_1 + \delta_{j1}\hat{p}, \hat{\rho}\hat{v}_j\hat{v}_2 + \delta_{j2}\hat{p}, \hat{\rho}\hat{v}_j\hat{v}_3 + \delta_{j3}\hat{p}, \hat{\rho}\hat{v}_j\hat{H}\right)^T, \\
\hat{v} &= \frac{\frac{\hat{v}_i}{\sqrt{T_i}} + \frac{\hat{v}_{i+1}}{\sqrt{T_{i+1}}}}{\frac{1}{\sqrt{T_i}} + \frac{1}{\sqrt{T_{i+1}}}}, \quad \hat{p} = \frac{\frac{\hat{p}_i}{\sqrt{T_i}} + \frac{\hat{p}_{i+1}}{\sqrt{T_{i+1}}}}{\frac{1}{\sqrt{T_i}} + \frac{1}{\sqrt{T_{i+1}}}}, \\
\hat{h} &= R\frac{\log\left(\frac{\sqrt{T_i}\rho_i}{\sqrt{T_{i+1}}\rho_{i+1}}\right)}{\frac{1}{\sqrt{T_i}} + \frac{1}{\sqrt{T_{i+1}}}}\left(\frac{\sqrt{T_i}\rho_i + \sqrt{T_{i+1}}\rho_{i+1}}{\left(\frac{1}{\sqrt{T_i}} + \frac{1}{\sqrt{T_{i+1}}}\right)\left(\sqrt{T_i}\rho_i - \sqrt{T_{i+1}}\rho_{i+1}\right)}\right. \\
&\qquad \left. + \frac{\gamma+1}{\gamma-1}\frac{\log\left(\sqrt{\frac{T_{i+1}}{T_i}}\right)}{\log\left(\sqrt{\frac{T_i}{T_{i+1}}}\frac{\rho_i}{\rho_{i+1}}\right)\left(\frac{1}{\sqrt{T_i}} - \frac{1}{\sqrt{T_{i+1}}}\right)}\right), \\
\hat{H} &= \hat{h} + \frac{1}{2}\hat{v}_\ell\hat{v}_\ell, \quad \hat{\rho} = \frac{\left(\frac{1}{\sqrt{T_i}} + \frac{1}{\sqrt{T_{i+1}}}\right)\left(\sqrt{T_i}\rho_i - \sqrt{T_{i+1}}\rho_{i+1}\right)}{2\left(\log(\sqrt{T_i}\rho_i) - \log(\sqrt{T_{i+1}}\rho_{i+1})\right)}.
\end{aligned} \tag{5.18}$$

This somewhat complicated explicit form is the first entropy conservative flux for the convective terms with low enough computational cost to be implemented in a practical simulation code. Previously, Tadmor [2] derived an entropy conservative flux form that required integration through phase space, but this was deemed too expensive to be practical.

5.1.4 Energy Stable Boundary Conditions

The problems studied herein are limited to open boundary conditions, which are implemented as suggested by Svärd et al. [28]

6 Accuracy Validation

The new entropy stable methodology is validated using linear advection, nonlinear Burgers' equation, the Euler equations, and the Navier-Stokes equations. The methodology is also extended to three dimensions for the compressible Euler and Navier-Stokes equations, the target applications for this work.

6.1 Test Equations

The accuracy and robustness of the algorithms developed herein are tested using two smooth and two discontinuous problems. The smooth problems are the propagation of an isentropic vortex, and the propagation of the viscous shock. Both problems demonstrate the design-order convergence of the new entropy conservative formulation.

6.1.1 Linear Advection

Linear advection tests the accuracy of the first derivative terms. Design order convergence of $p+1$ is sought in all cases. The linear advection equation is given by

$$\begin{array}{c} \frac{\partial u}{\partial t} \; + \; \frac{\partial c\, u}{\partial x} \; = \; 0 \quad ; \quad -1 \leq x \leq 1 \; ; \; t >= 0, \\ u(-1,t) = g_{-1}(t) \; , \end{array} \tag{6.1}$$

with an exact solution given by

$$u(x,t) \; = \; \exp(-\tfrac{1}{2}(x \; - \; ct)^2) \quad ; \quad c = 1 \quad . \tag{6.2}$$

Initial and boundary data is provided that is consistent with the exact solution.

6.1.2 Burgers' Equation

The nonlinear Burgers' equation is a one-dimensional model for the inviscid-viscous interaction found in the full Navier-Stokes equation. Burgers' equation is given by

$$\begin{array}{c} \frac{\partial u}{\partial t} \; + \; \frac{1}{2}\frac{\partial u^2}{\partial x} \; = \; \epsilon \frac{\partial^2 u}{\partial x^2} \quad ; \quad -1 \leq x \leq 1 \; ; \; t >= 0, \\ \alpha u(-1,t) - \epsilon u_x(-1,t) = g_{-1}(t) \; , \; \beta u(-1,t) + \epsilon u_x(-1,t) = g_{-1}(t) \; . \end{array} \tag{6.3}$$

An exact solution is given by

$$u(x,t) \; = \; \frac{a \exp((b-a)(x-ct-d)/(2\epsilon)+b}{1 \exp((b-a)(x-ct-d)/(2\epsilon)+1} \quad ; \quad a = -\tfrac{1}{2}, b = 1, c = \tfrac{1}{2}(a+b), d = \tfrac{1}{2} \tag{6.4}$$

Initial and boundary data are provided that is consistent with the exact solution.

6.1.3 Isentropic Vortex

The isentropic vortex is an exact solution to the Euler equations and is an excellent test of the accuracy and functionality of the inviscid components of a Navier-Stokes solver. It is fully described by

$$\begin{array}{rcl} f(x,y,z,t) & = & 1 - \left[(x - x_0 - U_\infty \cos(\alpha)\, t)^2 + (y - y_0 - U_\infty \sin(\alpha)\, t)^2 \right], \\ T(x,y,z,t) & = & \left[1 - \epsilon_v^2 M_\infty^2 \frac{\gamma-1}{8\pi^2} \exp\left(f(x,y,z,t) \right) \right], \quad \rho(x,y,z,t) \; = \; T^{\frac{1}{\gamma-1}}, \\ u(x,y,z,t) & = & U_\infty \cos(\alpha) - \epsilon_v \frac{y - y_0 - U_\infty \sin(\alpha) t}{2\pi} \exp\left(\frac{f(x,y,z,t)}{2} \right), \\ v(x,y,z,t) & = & U_\infty \sin(\alpha) - \epsilon_v \frac{x - x_0 - U_\infty \cos(\alpha) t}{2\pi} \exp\left(\frac{f(x,y,z,t)}{2} \right), \\ w(x,y,z,t) & = & 0. \end{array} \tag{6.5}$$

In this study the values $U_\infty \; = \; M_\infty c_\infty$, $\epsilon_v = 5.0$, $M_\infty = 0.5$, and $\gamma = 1.4$ are used.

The Cartesian grid test case is described by

$$x \in (-15, 15), \quad y \in (-15, 15), \quad (x_0, y_0) \; = \; (0,0), \quad \alpha = 0.0, \quad t \geq 0.$$

6.1.4 The Viscous Shock

The Navier-Stokes equations support an exact solution for the viscous shock profile, under the assumption that the Prandtl number is $Pr = \frac{3}{4}$. Mass and total enthalpy are constant across a shock. Furthermore, if $Pr = \frac{3}{4}$ then the momentum and energy equations are redundant. The single momentum equation across the shock is given by

$$\begin{gathered} \alpha v v_x - (v-1)(v-v_f) = 0 \quad ; \quad -\infty \leq x \leq \infty \quad , \quad t \geq 0; \\ v \;=\; \tfrac{u}{u_L} \;;\; v_f = \tfrac{u_R}{u_L} \;;\; \alpha \;=\; \tfrac{\gamma-1}{2\gamma}\tfrac{\mu}{Pr\,\dot{m}} \end{gathered} \tag{6.6}$$

An exact solution is obtained by solving the momentum equation for the velocity profile.

$$x \;=\; \tfrac{1}{2}\alpha\left(Log|(v-1)(v-v_f)| + \tfrac{1+v_f}{1-v_f}Log|\tfrac{v-1}{v-v_f}|\right) \tag{6.7}$$

A moving shock is recovered by applying a uniform translation to the solution. A full derivation of this solution appears in the thesis of Fisher [22].

6.2 Test Results

All tests include elements of polynomial degrees $1 \leq p \leq 4$. A uniform grid refinement study is performed using a grid-doubling procedure. When possible, a randomly distributed grid is used. A properly nested set of uniformly refined random grids is generated as follows. First, a random grid is generated at the coarsest resolution. This grid is then scaled and replicated 2^s, $3 \leq s \leq 8$ times on the interval $-1 \leq x \leq 1$. Thus, the randomness of the coarsest grid is preserved on all levels. All simulations use a fourth-order low-storage Runge-Kutta scheme to advance the solution in time. A temporal error controller is used to guarantee that the temporal error is subordinate to the spatial error, and to automate the determination of the maximum stable timestep for each test case.

6.2.1 Linear Advection

Table 1 provides data from a uniform grid refinement study of the linear advection equation. Design order convergence (i.e., $p+1$) is achieved in both the L_2 and L_∞ norms. This test verifies that the basic spectral collocation first derivative operator superconverges by one order, relative to the polynomial order of the approximation.

6.2.2 Nonlinear Burgers' Equation

Table 2 contains data from both a uniform and nonuniform grid refinement study of the nonlinear Burgers' equation. The nonuniform grid refinement study is included to identify superconvergence resulting from fortuitous cancellation of viscous error terms at element interfaces. (See reference [18] for a discussion of this phenomena.)

Sharp design order convergence of $p+1$ is achieved in both the L_2 and L_∞ norms on the uniform grid for polynomials of even order. This sharp convergence may be the result of fortuitous cancellation of errors. Design order convergence is achieved asymptotically for polynomials of odd order, in both L_2 and L_∞. The nonuniform refinement study shows asymptotic design order convergence for both even and odd polynomial orders.

This test verifies that the superconvergence observed in the linear advection study, extends to nonlinear inviscid terms, and that the entropy stable LDG implementation is design order accurate for the viscous terms. Furthermore, superconvergence may be achieved on irregular grids.

6.2.3 The Euler Vortex

The convergence rate for the isentropic Euler vortex is evaluated on a properly nested sequence of uniform two-dimensional grids. The vortex profile is initially located in the middle of the domain and is simulated until $t = 0.25$. The reference Mach number is $M = 0.5$, and the translation velocity of the vortex is unity. The errors for the uniform grids are shown in Table 3.

Theorem 3.4 proves that design order entropy conservative fluxes may be constructed using a linear combination of two-point entropy fluxes. A critical assumption used in the proof is that the two-point non-dissipative fluxes satisfy Tadmor's integral relation given in equation 3.18. Herein, the non-dissipative Euler fluxes of Ismail and Roe [13] are used. The study provides evidence that the non-dissipative Euler fluxes of Ismail and Roe [13] do not degrade the formal accuracy. The interfaces are treated by using the entropy stable characteristic fluxes with a weighting parameter tuned to produce "upwind fluxes" at the interfaces. Design order convergence is achieved in all cases.

6.2.4 The Viscous Shock

The convergence rate for the viscous shock is evaluated on a properly nested sequence of uniform and nonuniform grids. The shock profile is initially located in the middle of the domain and is simulated until $t = 1.00$. The Reynolds number is $Re = 10$ and the reference Mach number is $M = 2.5$. The errors for the uniform and the nonuniform grids are shown in Table 4.

The interfaces are treated by using the entropy stable characteristic fluxes with a weighting parameter tuned to produce "upwind fluxes" at the interfaces. Design order convergence is achieved in both the L_2 and L_∞ norms on uniform and nonuniform grids.

7 Conclusions

High-order entropy stable spectral collocation methods of arbitrary polynomial order, are derived for the nonlinear conservation laws of the Navier-Stokes equations. The discrete operators are formulated by representing conventional spectral operators in the summation-by-parts framework, for which entropy stability of the Navier-Stokes equations has already been established. The individual spectral elements are coupled together in an entropy stable and conservative fashion by using existing SBP-SAT operators for the convective terms. A new entropy stable local discontinuous Galerkin scheme is developed to couple the viscous terms. The new operators are shown to preserve design-order accuracy of $p + 1$ on model problems.

References

1. Randall LeVeque: *Numerical Methods for Conservation Laws*. Birkhauser, Basel, 1992.

2. Tadmor, E.: The numerical viscosity of entropy stable schemes for systems of conservation laws. I. *Mathematics of Computation*, vol. 49, 1987, pp. 91–103.

3. Harten, A.; Engquist, B.; Osher, S.; and Chakravarthy, S. R.: Uniformly high order accurate essentially non-oscillatory schemes, III. *Journal of Computational Physics*, vol. 71, no. 2, 1987, pp. 231–303. URL http://www.sciencedirect.com/science/article/pii/0021999187900313.

4. Shu, C.-W.; and Osher, S.: Efficient implementation of essentially non-oscillatory shock-capturing schemes. *Journal of Computational Physics*, vol. 77, no. 2, 1988, pp. 439–471. URL http://www.sciencedirect.com/science/article/pii/0021999188901775.

5. Liu, X.-D.; Osher, S.; and Chan, T.: Weighted Essentially Non-oscillatory Schemes. *Journal of Computational Physics*, vol. 115, no. 1, 1994, pp. 200–212. URL http://www.sciencedirect.com/science/article/pii/S0021999184711879.

6. Jiang, G.; and Shu, C.-W.: Efficient implementation of weighted ENO schemes. *Journal of Computational Physics*, vol. 126, 1996, pp. 202–228.

7. Qiu, J.-M.; and Shu, C.-W.: Convergence of Godunov-type schemes for scalar conservation laws under large time steps. *Siam Journal on Numerical Analysis*, vol. 46, 2008, pp. 2211–2237.

8. Yamaleev, N. K.; and Carpenter, M. H.: Third-order Energy stable WENO Scheme. *Journal of Computational Physics*, vol. 228, 2009, pp. 3025–3047.

9. Fisher, T. C.; and Carpenter, M. H.: High-order entropy stable finite difference schemes for nonlinear conservation laws: finite domains. TM-217971, NASA, 2013.

10. Fisher, T. C.; and Carpenter, M. H.: High-order entropy stable finite difference schemes for nonlinear conservation laws: finite domains. *Journal of Computational Physics*, vol. To Appear, 2013, p. ???

11. Tadmor, E.: Entropy stability theory for difference approximations of nonlinear conservation laws and related time-dependent problems. *Acta Numerica*, vol. 12, 2003, pp. 451–512.

12. LeFloch, P. G.; Mercier, J. M.; and Rohde, C.: Fully discrete, entropy conservative schemes of arbitrary order. *SIAM Journal on Numerical Analysis*, vol. 40, 2002, pp. 1968–1992.

13. Ismail, F.; and Roe, P. L.: Affordable, entropy-consistent Euler flux functions II: Entropy production at shocks. *Journal of Computational Physics*, vol. 228, 2009, pp. 5410–5436.

14. Fjordholm, U. S.; Mishra, S.; and Tadmor, E.: Arbitrarily high-order accurate entropy stable essentially nonoscillatory schemes for systems of conservation laws. *SIAM Journal on Numerical Analysis*, vol. 50, 2012, pp. 544–573.

15. Carpenter, M. H.; Nordström, J.; and Gottlieb, D.: A stable and conservative interface treatment of arbitrary spatial accuracy. *Journal of Computational Physics*, vol. 148, 1999, pp. 341–365.

16. Carpenter, M. H.; and Gottlieb, D.: Spectral methods on arbitrary grids. *Journal of Computational Physics*, vol. 129, 1996, pp. 74–86.

17. Hesthaven, J. S.; and Gottlieb, D.: A Stable Penalty Method for the Compressible Navier-Stokes Equations: I: Open Boundary Conditions. *SIAM Journal on Scientific Computing*, vol. 17, 1996, pp. 579–612.

18. Carpenter, M. H.; Nordström, J.; and Gottlieb, D.: Revisiting and Extending Interface Penalties for Multi-domain Summation-by-Parts Operators. *Journal of Scientific Computing*, vol. 45, 2009, pp. 118–150.

19. Gassner, G.: A skew-symmetric discontinuous Galerkin spectral element discretization and its relation to SBP-SAT finite difference methods. *SIAM Journal on Scientific Computing*, vol. 35, no. 3, 2013, pp. A1233–A1253.

20. Hughes, T.; Franca, L.; and Mallet, M.: A new finite element formulation for computational fluid dynamics: K. Symmetric forms of the compressible Euler and Navier-Stokes equations and the second law of thermodynamics. *Computer Methods in Applied Mechanics and Engineering*, vol. 54, 1986, pp. 223 – 234.

21. Hesthaven, J.; and Warburton, T.: *Nodal Discontinuous Galerkin Methods: Algorithms, Analysis, and Applications*. Texts in Applied Mathematics, Springer, 2008. URL http://books.google.com/books?id=APQkDOmwyksC.

22. Fisher, T. C.: High-order L^2 stable multi-domain finite difference method for compressible flows. Ph.D. Thesis, Purdue University, 2012.

23. Fisher, T. C.; Carpenter, M. H.; Nordström, J.; Yamaleev, N. K.; and Swanson, R. C.: Discretely conservative finite-difference formulations for nonlinear conservation laws in split form: theory and boundary conditions. TM 2011-217307, NASA, 2011.

24. Lax, P. D.: *Hyperbolic Systems of Conservation Laws and the Mathematical Theory of Shock Waves*. SIAM, Philadelphia, 1973.

25. Fisher, T. C.; Carpenter, M. H.; Nordström, J.; Yamaleev, N. K.; and Swanson, R. C.: Discretely conservative finite-difference formulations for nonlinear conservation laws in split form: theory and boundary conditions. *Journal of Computational Physics*, vol. 234, 2013, pp. 353–375.

26. Carpenter, M. H.; Gottlieb, D.; and Abarbanel, S.: Time-stable boundary conditions for finite-difference schemes solving hyperbolic systems: methodology and application to high-order compact schemes. *Journal of Computational Physics*, vol. 111, 1994, pp. 220–236.

27. Svärd, M.; and Nordström, J.: On the order of accuracy for difference approximations of initial-boundary value problems. *Journal of Computational Physics*, vol. 218, 2006, pp. 333–352.

28. Svärd, M.; Carpenter, M. H.; and Nordström, J.: A stable high-order finite difference scheme for the compressible Navier-Stokes equations, far-field boundary conditions. *Journal of Computational Physics*, vol. 225, 2007, pp. 1020–1038.

29. Nordström, J.; Gong, J.; van der Weide, E.; and Svärd, M.: A stable and conservative high order multi-block method for the compressible Navier-Stokes equations. *Journal of Computational Physics*, vol. 228, 2009, pp. 9020–9035.

30. Berg, J.; and Nordström, J.: Stable Robin solid wall boundary conditions for the Navier-Stokes equations. *Journal of Computational Physics*, vol. 230, 2011, pp. 7519–7532.

31. Kopriva, D. A.: *Implementing spectral methods for partial differential equations*. Springer, New York, 2009.

32. Godunov, S. K.: An interesting class of quasilinear systems. *Dokl. Akad. Nauk SSSR*, vol. 139, no. 3, 1961, pp. 521–523.

33. Mock, M. S.: Systems of Conservation Laws of Mixed Type. *Journal of Differential Equations*, vol. 37, 1980, pp. 70–88.

34. Harten, A.: On the Symmetric Form of Systems of Conservation Laws with Entropy. *Journal of Computational Physics*, vol. 49, 1983, pp. 151–164.

35. LeFloch, P. G.: *Hyperbolic Systems of Conservation Laws: The Theory of Classical and Non-classical Shock Waves*. Birkhäuser Verlag, Basel, 2002.

36. Arnold, D. N.; Brezzi, F.; Cockburn, B.; and Marini, L. D.: Unified analysis of discontinuous Galerkin methods for elliptic problems. *SIAM Journal on Numerical Analysis*, vol. 39(5), 2002, pp. 1749–1779.

37. Cockburn, B.; and Shu, C.: The local discontinuous Galerkin method for time-Dependent convection-diffusion systems. *SIAM Journal on Numerical Analysis*, vol. 35, no. 6, 1998, pp. 2440–2463. URL http://epubs.siam.org/doi/abs/10.1137/S0036142997316712.

38. Bassi, F.; and Rebay, S.: A high-order accurate discontinuous finite element method for the numerical solution of the compressible NavierStokes equations. *Journal of Computational Physics*, vol. 131, no. 2, 1997, pp. 267–279. URL http://www.sciencedirect.com/science/article/pii/S0021999196955722.

39. Merriam, M. L.: An Entropy-Based Approach to Nonlinear Stability. TM 101086, NASA, 1989.

Appendix A

Differentiation Operators

The discrete operators are provided for polynomial orders one to four in Table A1. Three quantities completely define the discrete operators; the diagonal norm, $\mathcal{P}$, the nearly skew-symmetric, $\mathcal{Q}$ and the positions of the collocation points, $\mathbf{x}$. (Recall the the differentiation matrix is defined as $D = \mathcal{P}^{-1}\mathcal{Q}$.) The upper triangular portion of $\mathcal{Q}$ is only provided. The full $\mathcal{Q}$ matrix may be reconstructed from the skew-symmetry property $\mathcal{Q} + \mathcal{Q}^T = \mathcal{B}$.

Table 1 Error convergence is shown for the linear advection equation.

P=1	L^2 error	L^2 rate	L^∞ error	L^∞ rate
8	3.41E-02		5.09E-02	
16	7.80E-03	-1.92	1.63E-02	-1.64
32	1.99E-03	-1.97	4.42E-03	-1.88
64	5.02E-04	-1.98	1.14E-03	-1.95
128	1.26E-04	-1.99	2.89E-04	-1.97
256	3.16E-05	-1.99	7.28E-05	-1.99
P=2	L^2 error	L^2 rate	L^∞ error	L^∞ rate
8	1.85E-03		2.64E-03	
16	2.46E-04	-2.90	3.46E-04	-2.93
32	3.12E-05	-2.97	4.69E-05	-2.88
64	3.91E-06	-2.99	5.99E-06	-2.97
128	4.89E-07	-2.99	7.56E-07	-2.98
256	6.12E-08	-2.99	9.62E-08	-2.97
P=3	L^2 error	L^2 rate	L^∞ error	L^∞ rate
8	5.28E-05		1.33E-04	
16	3.09E-06	-4.09	9.29E-06	-3.83
32	1.89E-07	-4.02	6.04E-07	-3.94
64	1.18E-08	-4.00	3.92E-08	-3.94
128	7.36E-10	-4.00	2.53E-09	-3.95
256	4.60E-11	-4.00	1.59E-10	-3.99
P=4	L^2 error	L^2 rate	L^∞ error	L^∞ rate
8	2.90E-06		5.62E-06	
16	9.12E-08	-4.99	1.92E-07	-4.87
32	2.83E-09	-5.00	6.02E-09	-4.99
64	8.81E-11	-5.00	1.86E-10	-5.01
128	2.77E-12	-4.99	5.79E-12	-5.00
256	1.17E-13	-4.56	5.45E-13	-3.40

Table 2 Error convergence is shown for the nonlinear Burgers' equation.

	Uniform Grid				Nonuniform Grid			
P=01	L^2 error	L^2 rate	L^∞ error	L^∞ rate	L^2 error	L^2 rate	L^∞ error	L^∞ rate
8	1.16E-02		2.40E-02		1.77E-02		2.94E-02	
16	4.43E-03	-1.38	9.67E-03	-1.31	5.65E-03	-1.64	1.25E-02	-1.24
32	1.55E-03	-1.51	3.56E-03	-1.44	1.87E-03	-1.59	4.36E-03	-1.51
64	4.94E-04	-1.65	1.19E-03	-1.57	5.66E-04	-1.72	1.41E-03	-1.62
128	1.46E-04	-1.75	3.74E-04	-1.67	1.66E-04	-1.76	4.56E-04	-1.62
256	4.13E-05	-1.82	1.13E-04	-1.73	4.69E-05	-1.82	1.35E-04	-1.75
512	1.13E-05	-1.86	3.29E-05	-1.77	1.29E-05	-1.86	3.99E-05	-1.76
1024	3.04E-06	-1.89	9.36E-06	-1.81	3.44E-06	-1.90	1.12E-05	-1.82
P=02								
8	1.00E-03		2.42E-03		2.04E-03		3.91E-03	
16	1.14E-04	-3.13	3.08E-04	-2.97	2.20E-04	-3.21	5.25E-04	-2.89
32	1.42E-05	-3.01	3.83E-05	-3.00	4.23E-05	-2.37	1.16E-04	-2.17
64	1.78E-06	-2.99	4.75E-06	-3.00	6.54E-06	-2.69	1.82E-05	-2.67
128	2.23E-07	-2.99	5.94E-07	-2.99	1.00E-06	-2.70	3.02E-06	-2.58
256	2.79E-08	-2.99	7.44E-08	-2.99	1.50E-07	-2.73	4.89E-07	-2.62
512	3.49E-09	-2.99	9.31E-09	-2.99	2.19E-08	-2.78	7.61E-08	-2.68
1024	4.36E-10	-2.99	1.16E-09	-2.99	3.07E-09	-2.83	1.14E-08	-2.73
P=03								
8	7.83E-05		2.01E-04		2.23E-04		5.16E-04	
16	7.87E-06	-3.31	2.41E-05	-3.05	2.26E-05	-3.30	5.69E-05	-3.18
32	7.55E-07	-3.38	2.30E-06	-3.38	1.49E-06	-3.92	4.47E-06	-3.66
64	6.79E-08	-3.47	2.09E-07	-3.46	1.26E-07	-3.56	4.02E-07	-3.47
128	5.68E-09	-3.57	1.76E-08	-3.57	1.04E-08	-3.59	3.30E-08	-3.60
256	4.43E-10	-3.67	1.38E-09	-3.66	8.05E-10	-3.68	2.62E-09	-3.65
512	3.26E-11	-3.76	1.02E-10	-3.75	5.91E-11	-3.76	1.95E-10	-3.74
1024	2.31E-12	-3.81	7.59E-12	-3.75	4.14E-12	-3.83	1.38E-11	-3.81
P=04								
8	5.51E-06		1.28E-05		1.26E-05		3.53E-05	
16	1.22E-07	-5.49	4.57E-07	-4.80	4.72E-07	-4.74	1.67E-06	-4.39
32	3.60E-09	-5.08	1.32E-08	-5.11	3.39E-08	-3.79	1.20E-07	-3.80
64	1.11E-10	-5.01	4.13E-10	-5.00	1.66E-09	-4.35	5.83E-09	-4.36
128	3.66E-12	-4.92	1.37E-11	-4.91	7.69E-11	-4.42	2.87E-10	-4.34
256	2.83E-13	-3.69	1.67E-12	-3.03	3.38E-12	-4.50	1.32E-11	-4.44
512	3.08E-14	-3.20	1.19E-13	-3.81	1.41E-13	-4.58	6.00E-13	-4.45
1024	3.65E-14	0.24	7.21E-14	-0.71	3.67E-14	-1.94	7.79E-14	-2.94

Table 3 Error convergence is shown for the isentropic Euler vortex equation.

	Uniform Grid			
P=01	L^2 error	L^2 rate	L^∞ error	L^∞ rate
04x02	1.42E-02		5.54E-02	
08x04	5.87E-03	-1.27	2.24E-02	-1.30
16x08	1.88E-03	-1.64	7.02E-03	-1.67
32x16	3.98E-04	-2.24	1.43E-03	-2.29
64x32	6.38E-05	-2.64	2.32E-04	-2.61
P=02				
04x02	1.83E-03		1.16E-02	
08x04	3.74E-04	-2.28	2.46E-03	-2.23
16x08	6.40E-05	-2.54	4.06E-04	-2.60
32x16	1.20E-05	-2.41	7.15E-05	-2.50
64x32	2.69E-06	-2.15	1.59E-05	-2.16
P=03				
04x02	1.43E-04		7.92E-04	
08x04	1.30E-05	-3.46	1.03E-04	-2.94
16x08	9.41E-07	-3.78	7.92E-06	-3.69
32x16	6.79E-08	-3.79	8.27E-07	-3.25
64x32	4.64E-09	-3.86	8.53E-08	-3.27
P=04				
04x02	1.02E-05		7.80E-05	
08x04	4.72E-07	-4.43	4.65E-06	-4.06
16x08	2.14E-08	-4.46	2.43E-07	-4.25
32x16	1.15E-09	-4.22	1.33E-08	-4.19
64x32	6.83E-11	-4.06	7.95E-10	-4.06

Table 4 Error convergence is shown for the Navier-Stokes equation.

	Uniform Grid				Nonuniform Grid			
P=01	L^2 error	L^2 rate	L^∞ error	L^∞ rate	L^2 error	L^2 rate	L^∞ error	L^∞ rate
4	1.95E-01		5.92E-01		4.14E-01		1.19E-00	
8	7.11E-02	1.46	2.73E-01	1.11	1.81E-01	1.19	7.30E-01	0.71
16	2.10E-02	1.76	9.51E-02	1.53	5.26E-02	1.78	2.52E-01	1.53
32	5.57E-03	1.92	2.57E-02	1.89	1.51E-02	1.80	8.85E-02	1.51
64	1.42E-03	1.97	6.50E-03	1.98	4.05E-03	1.91	2.40E-02	1.88
128	3.58E-04	1.99	1.63E-03	1.99	1.03E-03	1.97	6.06E-03	1.98
P=02								
4	2.64E-02		7.87E-02		1.02E-01		4.11E-01	
8	6.16E-03	2.10	3.04E-02	1.37	1.22E-02	3.07	5.04E-02	3.03
16	8.22E-04	2.91	4.13E-03	2.88	5.54E-03	1.14	3.74E-02	0.43
32	9.90E-05	3.05	8.73E-04	2.24	7.46E-04	2.89	7.41E-03	2.33
64	1.22E-05	3.02	1.09E-04	2.99	9.17E-05	3.03	8.78E-04	3.08
P=03								
4	8.08E-03		4.73E-02		1.54E-02		3.60E-02	
8	4.94E-04	4.03	3.93E-03	3.59	7.22E-03	1.09	5.53E-02	-0.62
16	3.45E-05	3.84	3.77E-04	3.38	3.86E-04	4.22	4.03E-03	3.78
32	2.12E-06	4.03	2.47E-05	3.93	2.89E-05	3.74	4.00E-04	3.34
64	1.28E-07	4.05	1.46E-06	4.08	1.76E-06	4.04	2.58E-05	3.95
P=04								
4	1.33E-03		7.03E-03		1.16E-02		8.84E-02	
8	8.24E-05	4.02	8.16E-04	3.11	1.12E-03	3.37	7.55E-03	3.55
16	2.35E-06	5.13	3.21E-05	4.67	7.72E-05	3.86	8.05E-04	3.23
32	7.15E-08	5.04	1.09E-06	4.88	2.23E-06	5.11	3.13E-05	4.69
64	2.21E-09	5.02	3.43E-08	4.99	6.92E-08	5.01	1.10E-06	4.83

Table A1 Differentiation operators for polynomials of degree one through four.

P =	1	P =	2	P =	3	P =	4
x1 =	-1	x1 =	-1	x1 =	-1	x1 =	-1
x2 =	+1	x2 =	0	x2 =	$-1/\sqrt{5}$	x2 =	$-\sqrt{3/7}$
		x3 =	+1	x3 =	$+1/\sqrt{5}$	x3 =	0
				x4 =	+1	x4 =	$+\sqrt{3/7}$
						x5 =	+1
p1 =	+1	p1 =	1/3	p1 =	1/6	p1 =	1 / 10
p2 =	+1	p2 =	4/3	p2 =	5/6	p2 =	49 / 90
		p3 =	1/3	p3 =	5/6	p3 =	32 / 45
				p4 =	1/6	p4 =	49 / 90
						p5 =	1 / 10
q11 =	-1/2	q11 =	-1/2	q11 =	-1/2	q11 =	-1/2
q12 =	+1/2	q12 =	2/3	q12 =	$(5/24\ (1 + \sqrt{5}))$	q12 =	$(7/120)\ (7+\sqrt{21})$
q22 =	+1/2	q13 =	-1/6	q13 =	$(-5/24\ (-1 + \sqrt{5}))$	q13 =	-(4/15)
		q22 =	0	q14 =	1/12	q14 =	$-(7/120)\ (-7+\sqrt{21})$
		q23 =	2/3	q22 =	0	q15 =	- 1/20
		q33 =	+1/2	q23 =	$(5\ \sqrt{5}/12)$	q22 =	0
				q24 =	$(5/24\ (1 - \sqrt{5}))$	q23 =	$(28\ \sqrt{7/3})/45$
				q33 =	0	q24 =	$-(49\ \sqrt{7/3})/180$
				q34 =	$(5/24\ (1 + \sqrt{5}))$	q25 =	$-(7/120)\ (-7+\sqrt{21})$
				q44 =	1/2	q33 =	0
						q34 =	$(28\ (\sqrt{7/3}))/45$
						q35 =	- 4/15
						q44 =	0
						q45 =	$(7/120)\ (7+\sqrt{21})$
						q55 =	1/2

REPORT DOCUMENTATION PAGE

Form Approved
OMB No. 0704-0188

1. REPORT DATE *(DD-MM-YYYY)*	2. REPORT TYPE	3. DATES COVERED *(From - To)*
01- 09 - 2013	Technical Memorandum	January 2013 - August 2013

4. TITLE AND SUBTITLE

Entropy Stable Spectral Collocation Schemes for the Navier-Stokes Equations: Discontinuous Interfaces

5a. CONTRACT NUMBER

5b. GRANT NUMBER

5c. PROGRAM ELEMENT NUMBER

6. AUTHOR(S)

Carpenter, Mark H.; Fisher, Travis C.; Nielsen, Eric J.; Frankel, Steven H.

5d. PROJECT NUMBER

5e. TASK NUMBER

5f. WORK UNIT NUMBER

794072.02.07.02.03

7. PERFORMING ORGANIZATION NAME(S) AND ADDRESS(ES)

NASA Langley Research Center
Hampton, VA 23681-2199

8. PERFORMING ORGANIZATION REPORT NUMBER

L-20317

9. SPONSORING/MONITORING AGENCY NAME(S) AND ADDRESS(ES)

National Aeronautics and Space Administration
Washington, DC 20546-0001

10. SPONSOR/MONITOR'S ACRONYM(S)

NASA

11. SPONSOR/MONITOR'S REPORT NUMBER(S)

NASA/TM-2013-218039

12. DISTRIBUTION/AVAILABILITY STATEMENT

Unclassified - Unlimited
Subject Category 02
Availability: NASA CASI (443) 757-5802

13. SUPPLEMENTARY NOTES

14. ABSTRACT

Nonlinear entropy stability and a summation-by-parts framework are used to derive provably stable, polynomial-based spectral collocation methods of arbitrary order. The new methods are closely related to discontinuous Galerkin spectral collocation methods commonly known as DGFEM, but exhibit a more general entropy stability property. Although the new schemes are applicable to a broad class of linear and nonlinear conservation laws, emphasis herein is placed on the entropy stability of the compressible Navier-Stokes equations.

15. SUBJECT TERMS

Energy estimate; Entropy stability; LDG; Local discontinuous Galerkin; Numerical stability; Spectral collocation

16. SECURITY CLASSIFICATION OF:			17. LIMITATION OF ABSTRACT	18. NUMBER OF PAGES	19a. NAME OF RESPONSIBLE PERSON
a. REPORT	b. ABSTRACT	c. THIS PAGE			STI Help Desk (email: help@sti.nasa.gov)
					19b. TELEPHONE NUMBER *(Include area code)*
U	U	U	UU	40	(443) 757-5802